Energy & Environmental Science

ROYAL SOCIETY
OF **CHEMISTRY**

REVIEW ARTICLE
Xueliang Sun, Jian Peng *et al.*
Reviving ether-based electrolytes for sodium-ion batteries

Check for updates

Reviving ether-based electrolytes for sodium-ion batteries

Fangyuan Cheng,[abc] Jun Hu,[d] Wen Zhang,[abc] Baiyu Guo,[ac] Peng Yu,[d] Xueliang Sun [ID] *[ac] and Jian Peng [ID] *[ac]

The development of ether-based electrolytes has significant challenges, primarily caused by the irreversible co-intercalation of ether and Li$^+$ into commercial graphite, which excluded ether from use in commercial lithium-ion batteries (LIBs). However, the explosive development of sodium-ion batteries (SIBs) in recent years has driven a revival in ether-based electrolytes, due to their superior rate capability and low temperature suitability. In this review, we trace the evolution of ether-based electrolytes, from rise and subsequent decline to their current revival. We provide comprehensive analysis of the compatibility mechanisms between ether-based electrolytes and both anodes and cathodes in SIBs. Furthermore, we assess the feasibility of commercializing ether-based electrolytes, considering key factors such as electrochemical performance, safety and cost. Finally, we highlight critical challenges that must be overcome, from fundamental research to large-scale commercialization, and provide theoretical guidance for future development and innovation of ether-based electrolytes.

Broader context

Ether-based electrolytes have been developed rapidly in the last three years due to their unique "Na$^+$–solvent" effects and low reduction potential, making them well adapted to sodium-ion batteries (SIBs), which is crucial for optimizing low-temperature and rate performance of SIBs. In addition, ether-based electrolytes are one of the best choices for next-generation ultra-low temperature electrolytes due to their moderate solvation capability. However, the oxidative stability and safety of ether solvents have raised concerns in their commercialization. This review traces the evolution of ether-based electrolytes, from their rise and subsequent decline to their current revival, and new insights are provided at the end. Moreover, the potential for commercial application of ether-based electrolytes for SIBs is comprehensively evaluated based on electrochemical performance, safety and cost. Finally, we discuss the challenges that must be addressed for ether-based electrolytes to transition from fundamental research to commercial applications.

1. Introduction

Energy storage is significant for the development of low-carbon and zero-carbon power systems; however, the widespread deployment of lithium-ion batteries (LIBs) for large-scale energy storage is constrained by the limited availability of lithium resources.[1] Sodium-ion batteries (SIBs), which share similar compositions and reaction mechanisms with LIBs,[2] are emerging as promising alternative energy storage systems. SIBs benefit from a natural cost advantage due to the abundance and wide distribution of sodium,

and low temperature tolerance due to the small Na$^+$ Stokes radius and high reactivity,[3–5] positioning them as an effective complement to LIBs and a key player in the broader energy storage industries.

Throughout the development of LIBs, the electrolyte has played a decisive role, affecting the capacity, cycle life, rate performance, temperature tolerance and safety of batteries. The commercialized LiCoO$_2$ cathode was first produced in 1980[6] and commercialized carbon-based anodes were first produced in 1985,[7,8] but it was the emergence of ethylene carbonate (EC)-based electrolytes in the 1990s, suitable for both cathodes and anodes, that enabled the successful commercialization of LIBs.[9,10] For decades, challenges related to the instability between graphite and propylene carbonate (PC) hindered progress due to a lack of understanding of the interphase.[9,11,12] Therefore, drawing from the experience with LIBs, it is clear that the electrolyte must be regarded as a central focus in the development of SIBs, transitioning from a passive response to

[a] Eastern Institute for Advanced Study, Eastern Institute of Technology, Ningbo, 315200, China. E-mail: xsun@eitech.edu.cn, jpeng@eitech.edu.cn

[b] School of Chemistry and Materials Science, University of Science and Technology of China, Hefei, 230026, China

[c] Ningbo Key Laboratory of All-Solid-State Battery, Ningbo, 315200, China

[d] State Key Laboratory of Material Processing and Die & Mould Technology, School of Materials Science and Engineering, Huazhong University of Science and Technology, Wuhan, 430074, P. R. China

6874 | *Energy Environ. Sci.*, 2025, **18**, 6874–6898

This journal is © The Royal Society of Chemistry 2025

demand to an active driver of breakthrough innovations. Efforts must be made to explore high-performance electrolytes and accelerate the commercialization of SIBs.

Among the most promising electrolytes for SIBs are both ester-based electrolytes and ether-based electrolytes. While ester-based electrolytes are commercially used in LIBs, ether–Li$^+$ co-embedding in graphite leads to structural disruption, preventing ether from being used in commercialized LIBs.[13–16] Hard carbon (HC) is considered a promising anode for commercial application in SIBs, but the poor kinetics of the ester-based electrolyte fail to meet the low-temperature and fast charging requirements.[17,18] Notably, HC contains graphite-like microcrystallites and open angular microcrystallites, which enable the co-embedding of ether and Na$^+$ with high reversibility.[19–21] Moreover, the solvation binding between the cyclic ether–Na$^+$ is weaker than that of the cyclic ester and Na$^+$, promoting a faster desolvation of Na$^+$.[22–24] Equally important, the lowest unoccupied molecular orbital (LUMO) energy level of ether is higher than that of ester, making it more resistant to reduction and better adapted to the low-voltage anode.[25–28] These advantages position ether as a competitive candidate for enhancing the kinetic performance of SIBs, and ether-based electrolytes have flourished in recent years.

As the quest for preeminent ether-based electrolytes continues, there is an urgent need to review the state-of-the-art ether-based electrolytes from fundamental research to commercial applications (Fig. 1). Herein, we provide a comprehensive analysis of the characteristics of high-performance ether-based electrolytes and the compatible mechanisms by which ether interacts with anodes and cathodes in SIBs, and explore the development of novel ether solvents. Moreover, the potential for commercial applications of ether-based electrolytes in SIBs is comprehensively evaluated based on the electrochemical performance, safety and cost. Finally, we discuss the challenges that must be addressed for ether-based electrolytes to transition from fundamental research to commercial applications. These challenges include validating high-capacity full-battery performance (such as high-voltage resistance and safety), exploring innovative mechanisms, and developing novel high-performance ethers. The aim of this review is to stimulate further research into the practical applications of ether-based electrolytes and to achieve the development of ether-based electrolytes that combine both excellent kinetic and thermodynamic properties, ultimately facilitating the rapid application of SIBs in the energy storage market.

2. Key parameters required for high-performance ether-based electrolytes

As indispensable and ubiquitous components, electrolytes play a pivotal role in not only transporting Na$^+$, but also expanding the electrochemical stability window, suppressing side reactions and manipulating the redox mechanism. All of these are closely associated with the behavior of solvation chemistry within electrolytes.[29–31] It is indisputable that high-performance electrolytes are indispensable for realizing high-performance SIBs.

Generally, ether-based electrolytes used for SIBs must possess four characteristics (Fig. 2). Firstly, the basic function of an electrolyte is to transport Na$^+$ between the cathode and anode. Ether, as an electrolyte solvent, must have low viscosity, high

Fangyuan Cheng She is a post-doctoral researcher at Eastern Institute of Technology, Ningbo. She earned her PhD degree from Huazhong University of Science and Technology in 2024, following her Bachelor's degree from Hefei University of Technology in 2018. Her primary research focus is on the electrolyte and interface modification for lithium/sodium-ion batteries.

Fangyuan Cheng

Xueliang Sun He is a Chair Professor at Eastern Institute of Technology, Ningbo, and a Foreign Member of the Chinese Academy of Engineering. He is a Fellow of both the Canadian Academy of Engineering and the Royal Society of Canada, as well as the founding Editor-in-Chief of Electrochemical Energy Reviews. His research focuses on advanced materials for electrochemical energy storage and conversion, including all-solid-state batteries, lithium-ion batteries, and sodium-ion batteries.

Xueliang Sun

Jian Peng He is an Assistant Professor at the Eastern Institute of Technology, Ningbo. He earned his PhD degree from the University of Wollongong in 2022, and Master's degree from Huazhong University of Science and Technology in 2018. He has undertaken postdoctoral research at Western University. He is primarily engaged in the research of key materials and advanced characterization techniques for all-solid-state sodium batteries.

Jian Peng

This journal is © The Royal Society of Chemistry 2025

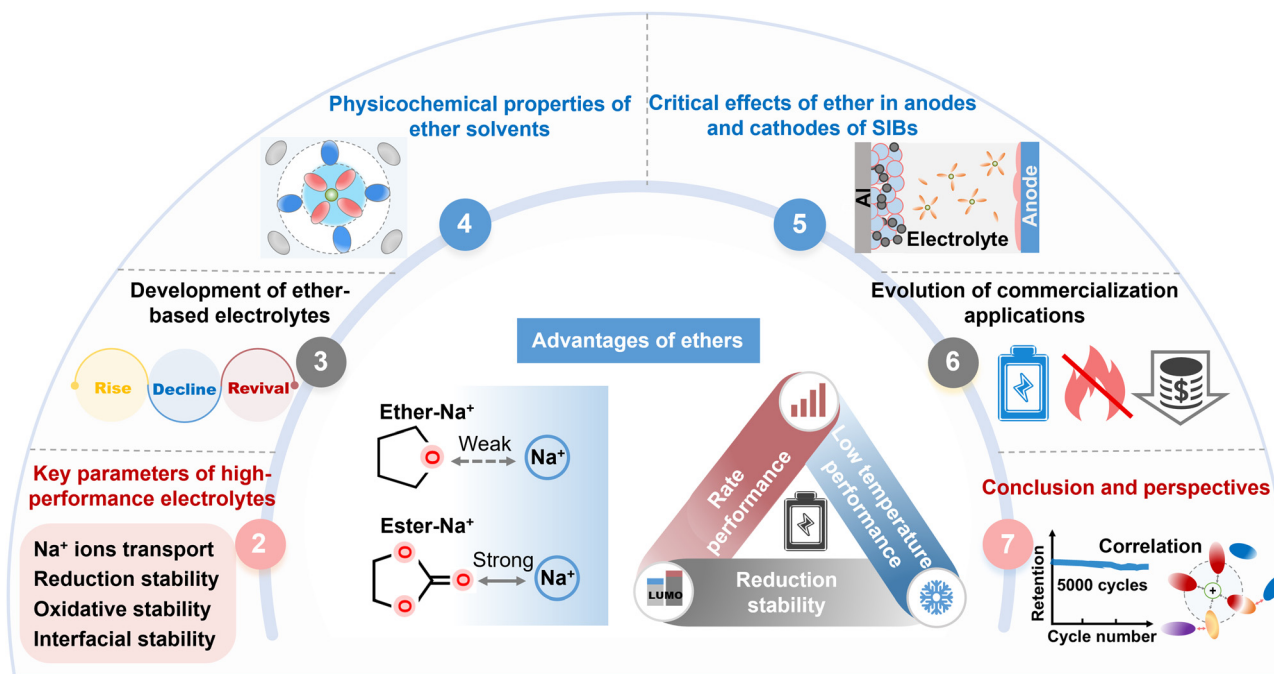*Energy Environ. Sci.*, 2025, **18**, 6874–6898 | **6875**
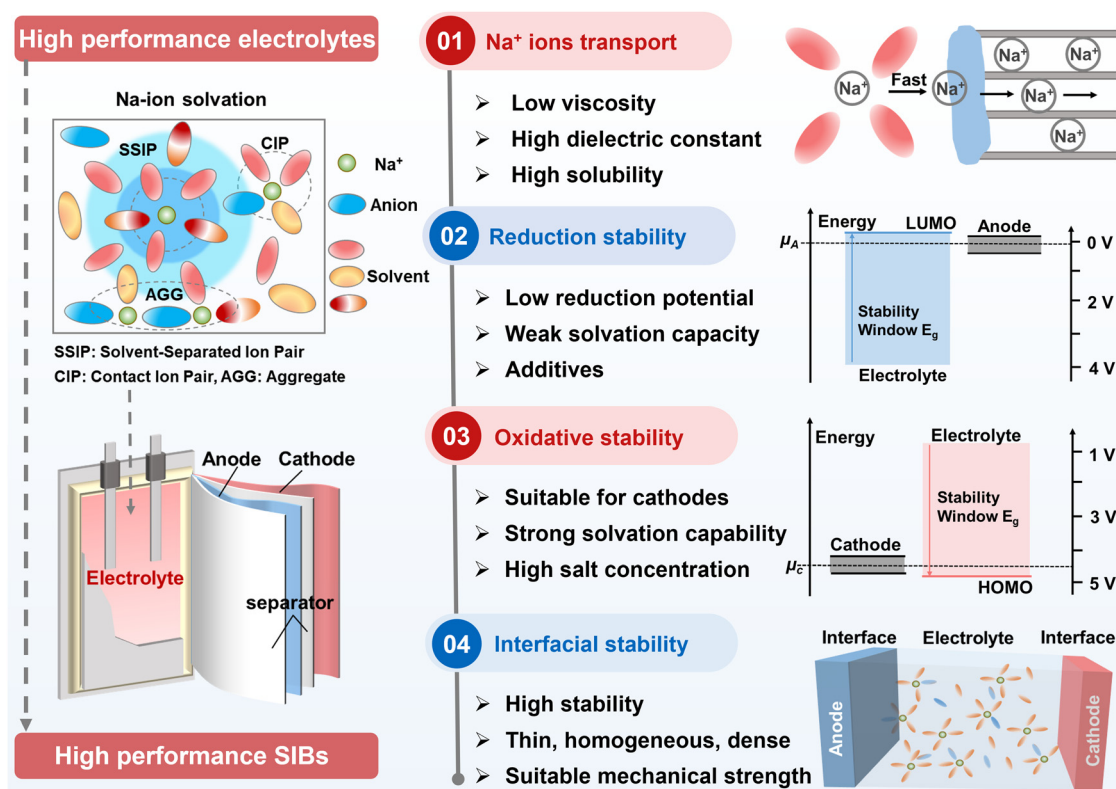
Fig. 1 The main points of this review.

Fig. 2 Characteristics required for high-performance ether-based electrolytes in SIBs.

dielectric constant and high sodium salt solubility to ensure a high Na$^+$ conductivity. Secondly, the highest occupied molecular orbital (HOMO) energy level[25,32] reflects the oxidative stability of the molecule. Ether-based electrolytes require high oxidative stability to match high-voltage cathodes, which can be achieved by lowering the HOMO energy level of the ether or by

6876 | Energy Environ. Sci., 2025, **18**, 6874–6898

This journal is © The Royal Society of Chemistry 2025

forming a strong solvation bond with Na$^+$ to reduce the HOMO energy level, as well as through the formation of a highly concentrated salt electrolyte to reduce the percentage of free ether.[33,34] Thirdly, the LUMO energy level reflects the reduction stability of the molecule, and the higher LUMO energy level denotes better reduction stability.[27,35,36] Ether-based electrolytes ought to obtain high reduction stability to match low-voltage anodes. This can be achieved by having a high LUMO energy level, or forming a weak solvation bond with Na$^+$ to minimize the LUMO energy level of the ether.[37,38] The interaction between cations and solvents usually strengthens the oxidation stability and weakens the reduction stability of the solvents. In contrast, further incorporation of anions into the cation–solvent complex has the opposite effect, significantly influencing the interfacial stability and the corresponding cycling lifespan.[39,40] Finally, high electrode–electrolyte interface stability is crucial to prevent interfacial parasitic reactions.[41] The interphase is the most important yet least understood component.[41–44] The cathode–electrolyte interphase (CEI)/solid–electrolyte interphase (SEI) derived from ether-based electrolytes must possess high antioxidant/reducing ability, and be thin, uniform, dense and exhibit moderate mechanical strength to ensure that the interface film is chemically and electrochemically stable and resistant to cracking.[45,46] Apart from the above basic properties, high thermal stability and wide liquid range also significantly impact the high- and low-temperature performance of batteries.[47,48] However, complex solvent chemistry and the complicated coupling effect between solvents and ions lead to the lack of perfect electrolytes. Therefore, decoupling the ''structure–property–performance'' constitutive relationship in electrolytes is crucial.

3. Development of ether-based electrolytes

Comprehensively understanding the development history of ether in electrolytes is important for guiding future development. Here, we critically reviewed the journey of ether-based electrolytes, from their emergence and decline to their recent revival. Typically, ether-based electrolytes consist of three parts: ether solvent, sodium salt and functional additives, each contributing to the properties of the electrolyte. Among these, ether solvent accounts for approximately 85 wt% (Fig. 3(a), mass ratio) and plays a decisive role in the battery performance. Currently, commercialized LIB electrolytes use ester as the solvent. Compared to ester, ethers have both advantages and disadvantages (Fig. 3(b)). Specifically, ether-based electrolytes
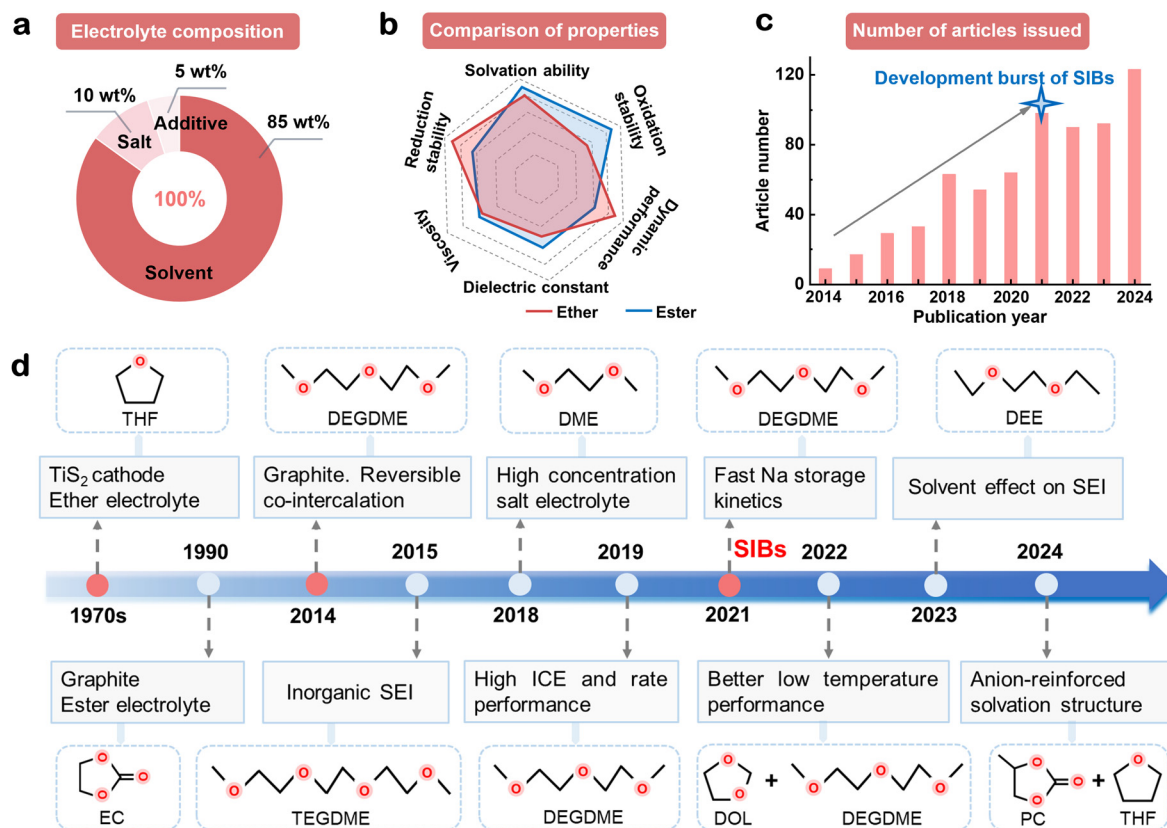
Fig. 3 Key properties and development of ether-based electrolytes. (a) Composition of ether-based electrolyte. (b) Comparison of ether and ester properties. (c) The number of publications dealing with ether-based electrolytes for sodium batteries from 2014 to November 2024 (data collected via the Web of Science by searching with ether and sodium battery as key words). (d) A timeline showing the development of ether-based electrolytes with the important milestones.

have obvious advantages in reduction stability and kinetic performance but are inferior in oxidative stability. These differences are triggered by the different front-line molecular orbital energy levels and solvation environments of ether and ester. According to the theory of front-line molecular orbital energy levels, the outmost electrons in the orbitals are preferentially involved in the reaction.[49,50] Ethers have higher LUMO and HOMO energy levels than esters, exhibit better resistance to reduction but worse resistance to oxidation. Esters are successfully applied in commercialized LIB electrolytes because their inferior reduction stability is compensated by their ability to form a robust anode–electrolyte interphase. For solvation environments, the cyclic esters have more negative charges on the carbonyl oxygen atoms, resulting in stronger interactions with Na^+ and slower desolvation, resulting in inferior kinetics compared to cyclic ethers.[22,51]

The past decade has witnessed a surge in research on ether-based electrolytes for SIBs, with a sharp increase in publications around 2021 (Fig. 3(c)). Recently, CATL, a leading power battery company, held a sodium-ion battery conference showcasing Prussian white and HC SIBs with energy densities up to 160 W h kg^{-1}. The industrialization of sodium-ion batteries will be achieved in the coming years, which marks the beginning of an explosive growth period in SIBs. The outstanding compatibility between ether-based electrolytes and HC drives the rapid development of ether-based electrolytes.[52] From 2021 to 2024, ether-based electrolytes entered a period of rapid and stable development.

The development of ether-based electrolytes is strongly dependent on the anodes and cathodes of batteries (Fig. 3(d)). Whittingham proposed the first intercalation cathode (TiS_2) in 1970s, and an ether-based electrolyte comprising $LiClO_4$ in dimethyl ether (DME)/tetrahydrofuran (THF) was employed due to the moderate working potential of TiS_2 (<3.0 V vs. Li/Li^+), which was in the stable range of ether-based electrolytes.[53] In the 1990s, graphite became commercial anode for LIBs by chemically forming the graphite intercalation compound LiC_6.[9] In order to use LiC_6 as an anode for rechargeable batteries, it is necessary to electrochemically form it in an electrolyte system. Simultaneously, realizing LiC_6 as an anode for rechargeable batteries required an electrolyte compatible with the high-voltage $LiCoO_2$ cathode (>4.0 V, vs. Li/Li^+).[54] Ether-based electrolytes were excluded from commercial LIB systems due to their low upper voltage window and structural damage caused by co-intercalation with Li^+ in graphite, therefore their development was impeded. In 2000, Stevens and Dahn discovered HC with excellent Na^+ intercalation properties,[55] which became a major turning point in the field of SIBs. However, the immaturity of the SIB research system at that time limited its impact on the commercialization of SIBs.

Another major turning point occurred in 2014 with the discovery that modulation of the solvation structure of ether-based electrolytes could achieve reversible co-embedding of diethylene glycol dimethyl ether (DEGDME) and Na^+ in graphite, realizing highly efficient Na^+ storage behavior for graphite.[15,56] Specifically, irreversible co-embedding can be circumvented through co-intercalation progress in a DEGDME-based electrolyte,

forming a ternary intercalation compound with an estimated stoichiometry of Na(DEGDME)$_2$C$_{20}$. From 2015 to 2020, the superior compatibility of ether-based electrolytes with sodium metal anodes and HC anodes was achieved respectively, mainly focusing on linear ethers such as DME, DEGDME and tetraethylene glycol dimethyl ether (TEGDME).[57–63] These electrolytes exhibited advantages such as high first initial coulombic efficiency (ICE), excellent rate performance and low-temperature performance. By 2021,[64] the development of SIBs entered into an explosive period, accelerating significant progress in novel ether-based electrolytes. From 2021 to 2024,[65–69] substantial research efforts emerged, focusing on designing innovative ethers and regulating electrolyte solvation structures. Recent advancements have introduced a range of novel ether compounds, including 1,2-diethoxyethane (DEE), 1,3-dioxolane (DOL), 2-methyl tetrahydrofuran (2-MTHF), hexafluoroisopropyl methyl ether (HFME), bis(2,2,2-trifluoroethyl) ether (BTFE), 1,2-bis(1,1,2,2-tetrafluoroethoxy) ethane (TFEE), 1H,1H,5H-octafluoropentyl-1,1,2,2-tetrafluoroethyl ether (OTE), 1,1,2,2-tetrafluoroethyl-2,2,3,3-tetrafluoropropyl ether (TTE), etc. These compounds, with diverse structural characteristics, have created various solvent effects, driving battery performance to new heights and further offering ether-based electrolytes great potential for commercial applications.[70–75]

4. Physicochemical properties of ether solvents

The physicochemical properties of ethers as electrolyte solvents affect the composition and structure of the electrode–electrolyte interphase, as well as the desolvation ability of Na^+. These properties directly determine the electrochemical stability window, cycle life, rate performance, high/low-temperature performance and safety performance of batteries.[76,77] Key attributes of ethers include their dielectric constant, melting point, boiling point, redox stability and electron donor number.[78,79]

The melting and boiling points of solvents significant impact the high/low-temperature performance and safety performance of batteries.[80] The melting and boiling points of ethers, esters, sulfites, sulfones and carboxylates are summarized in Fig. 4(a),[81,82] and the chemical names and corresponding abbreviations are displayed in Table 1. Solvents with lower melting points are less likely to solidify at low temperatures, allowing the electrolyte to remain fluid. This ensures that batteries can still be charged and discharged normally at low temperatures, avoiding the performance degradation caused by electrolyte solidification.[17,18] Ethers with lower melting point, such as THF, 2-MTHF, TTE, and OTE, exhibit superior low-temperature performances compared to esters, similar to the sulfate solvents like dimethyl sulfite (DMS) and diethyl sulfite (DES), as well as carboxylates. Conversely, solvents with high-boiling points maintain stability under normal operating conditions, resist evaporation, and prevent safety issues such as increased battery pressure, swelling or catastrophic failure.[31,79] However, most ethers, despite their advantages, have a low boiling point, which may pose safety risks.

6878 | Energy Environ. Sci., 2025, **18**, 6874–6898

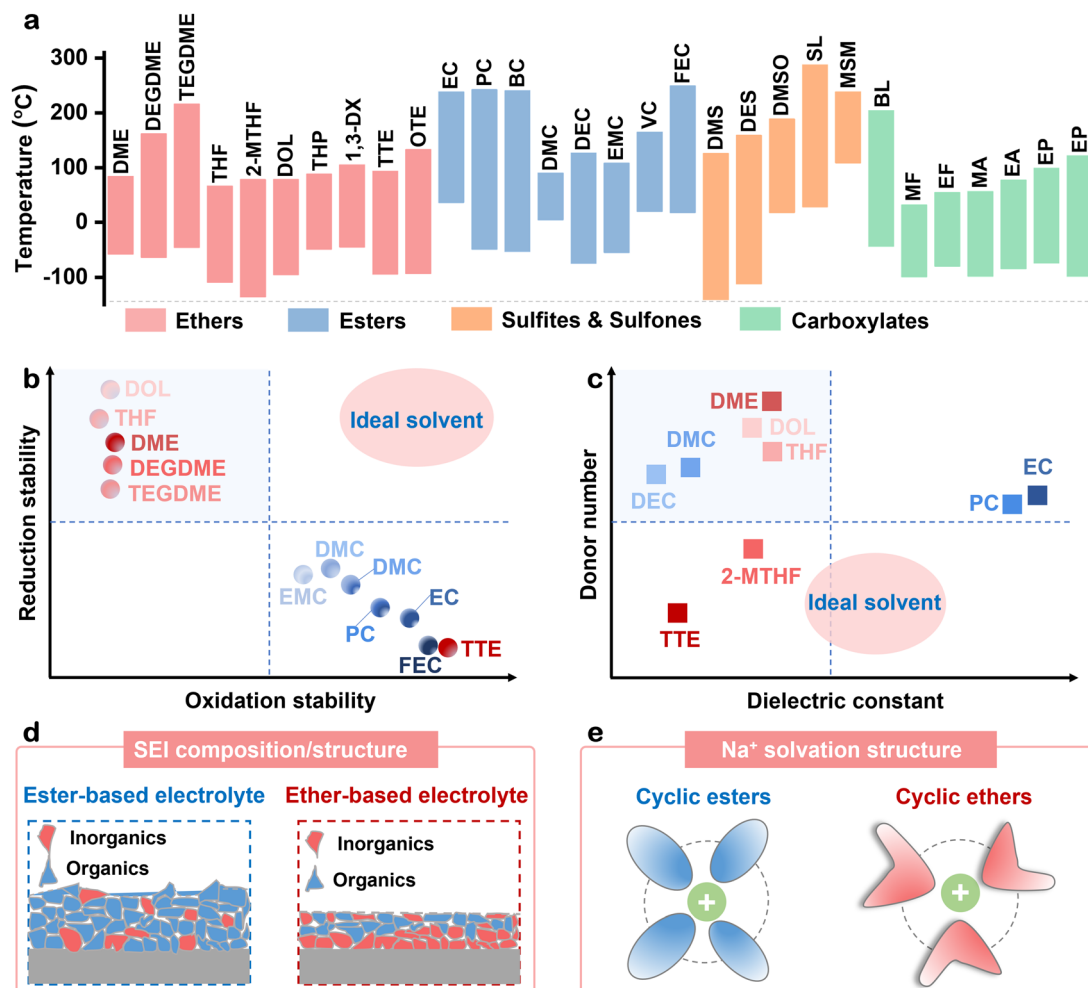This journal is © The Royal Society of Chemistry 2025

Fig. 4 (a) Summary of liquid ranges of popular solvents. (b) Oxidation stability and reduction stability of ethers and esters. (c) Dielectric constant and donor number of ethers and esters. (d) SEI composition/structure in ester- and ether-based electrolytes. (e) Na$^+$ solvation structure in ester- and ether-based electrolyte.

Table 1 Chemical name and the corresponding abbreviation of solvents

Chemical name	Abbreviation	Chemical name	Abbreviation	Chemical name	Abbreviation
Dimethyl ether	DME	Diethylene glycol dimethyl ether	DEGDME	Tetraethylene glycol dimethyl ether	TEGDME
Tetrahydrofuran	THF	2-Methyl tetrahydrofuran	2-MTHF	1,3-Dioxolane	DOL
Tetrahydropyran	THP	1,3-Dioxane	1,3-DX	1,1,2,2-Tetrafluoroethyl-2,2,3,3-tetrafluoropropyl ether	TTE
1H,1H,5H-Octafluoropentyl-1,1,2,2-tetrafluoroethyl ether	OTE	Ethylene carbonate	EC	Propylene carbonate	PC
Butenyl carbonate	BC	Dimethyl carbonate	DMC	Diethyl carbonate	DEC
Methyl ethyl carbonate	EMC	Vinyl Carbonate	VC	Fluoroethylene carbonate	FEC
Dimethyl sulfite	DMS	Diethyl sulfite	DES	Dimethyl sulfoxide	DMSO
Sulfolane	SL	Methyl sulfone	MSM	Gamma-butyrolactone	GBL
Methyl formate	MF	Ethyl formate	EF	Methyl acetate	MA
Ethyl acetate	EA	Ethyl propionate	EP	Ethyl butyrate	EB

The redox stability of solvents is a critical factor affecting the electrochemical stability window of electrolytes.[83] The cycle life of batteries can be significantly improved by rational selection and design of solvents. Ideal solvents should exhibit both high oxidation and reduction stability, as shown in Fig. 4(b),[84–86] but ethers generally possess high reduction stability but

lack oxidation stability, whereas esters show the opposite behavior.[23] The LUMO energy levels of most solvents decrease after coordination with Na$^+$, which indicates a decrease in the reductive stability of the solvent.[87] This decrease is related to factors such as the binding energy, bond length and orbital ratio of the solvent molecules. In particular, the decrease in the

LUMO energy level is more pronounced in cyclic ethers, which may be related to their molecular structure and electronic properties.

Most of the known polar solvents with high salt dissociation ability have high dielectric constants and high donor number values,[88,89] such as EC and PC,[90,91] whereas those with low dielectric constants and low donor number, such as TTE, have poor salt dissociation ability and represent non-solvation diluents (Fig. 4(c)). However, there seems to be a sweet spot consisting of a group of solvents with moderate dielectric constants and low donor number values, which leads to moderate Na$^+$ solvent binding energy and salt dissociation ability. For instance, methyl 2,2-difluoro-2 (fluorosulfonyl) acetate (MDFSA)[92] demonstrates compatibility with extreme conditions, such as high-voltage, ultra-low-temperature and high-rate simultaneously, showcasing the potential of such solvents to satisfy a range of demanding performance criteria.

Ethers and esters, due to their distinct physicochemical properties, result in different SEI compositions and solvation structures, leading to variations in the electrochemical performance of the batteries. Ethers and esters, due to their distinct physicochemical properties, result in different SEI compositions and structures, leading to variations in the electrochemical performance of the batteries. Compared with EC/DEC-based electrolyte, DEGDME shows a high solvation energy and reduction stability. Hence, there is a preferential reduction of NaPF$_6$, forming an inorganics-dominant SEI. Different from the DEGDME system, the carbonate solvents will undergo severe decomposition to form a thicker SEI.[23] Specifically, the carbonate-based electrolyte exhibits higher content of carbonyl and carboxyl species compared to the ether-based electrolyte. Furthermore, the ether-based electrolyte exhibits a higher concentration of Na–O, Na–PFO, and Na–F, while the carbonate-based electrolyte predominantly shows Na–CO$_3$. Similarly, fluorine and phosphorous exhibit increased content in the ether-based electrolyte, with the dominant species of Na–F, Na–PO$_x$F$_y$, and –PF$_5$.[93] NaF, present in the SEI layer close to the electrode surface, plays a crucial role in inhibiting the growth of sodium dendrites.[94,95] In brief, ether-based electrolytes tend to produce thin SEIs enriched with inorganic components (Fig. 4(d)). The solvation interaction between Na$^+$ and ethers is weaker than that between Na$^+$ and ester.[21,96,97] Modulating the Na$^+$ solvation structure is a key strategy for improving battery performance. On the one hand, it regulates the coordination between the solvent and Na$^+$ and improves the Na$^+$ desolvation kinetics.[98] On the other hand, it facilitates the optimization of the SEI/CEI composition, thereby enhancing the electrochemical performance of SIBs.[99]

The primary criteria for solvent selection include a low freezing point, moderate boiling point, wide electrochemical stability window, high dielectric constant and moderate donor number. These properties collectively ensure a high-performance electrolyte with stabilized CEI/SEI and low Na$^+$ desolvation energy. However, achieving all these requirements simultaneously remains challenging. For example, solvents with a higher the boiling point often have a lowered melting point. In practice, mixed solvents are usually used to make up for the shortcomings of each solvent, achieving a balance between these critical properties.

A comprehensive understanding of the interactions between ethers and cations/anions is a prerequisite for regulating the solvation chemistry in liquid electrolytes.[37,100–102] Typically, solvent–Na$^+$, solvent–solvent and solvent–anion interactions co-exist in the electrolytes. These interactions are highly important for expanding the electrochemical stability window, manipulating kinetics, regulating reaction mechanisms and suppressing side reactions in batteries.[82,103,104] For instance, the relative affinity intensity of solvent–Na$^+$ determines the solubility of sodium salt. More importantly, the relative interaction intensity of the complexes determines the solvation structures of Na$^+$.

In Fig. 5(a), strong electrostatic interactions between solvent–Na$^+$ promote the derivation of strongly solvated structures, which facilitate the dissolution of sodium salts, reduce the HOMO energy level of the solvent, and enhance oxidative stability. Regrettably, these strong interactions also reduce the LUMO energy level of the solvent and diminish the reduction stability. In addition, a strong solvation structure can hinder the desolvation behavior of Na$^+$. The strong solvation between solvent–Na$^+$ can be attenuated by dipole–dipole interactions between solvent–solvent in Fig. 5(b). Solvents with this characteristic, called diluents, do not participate in the Na$^+$ solvation structure but instead interact with primary solvent to enhance the kinetic properties. The electrostatic interactions between solvent–anion (Fig. 5(c)) have received less attention because solvents generally exhibit stronger preference for coordinating with Na$^+$ compared to the large anions, consequently, the ion mobility of the electrolyte is primarily governed by the free anions rather than by Na$^+$. Adjusting the solvent structure to enhance the interaction between the solvent and anions and simultaneously freeing Na$^+$ from the strongly solvated structure is crucial for enhancing the Na$^+$ mobility and desolvation behavior. Although anion solvation is weaker compared to cation solvation, the outermost orbitals of the anions can interact more strongly with the surrounding solvent because the valence electron density of the anions is more dispersed than that of the cations. Further research is still needed to understand how the anion solvation structures affect the properties of the electrolyte, alter the interfacial reaction paths, and influence the electrochemical performance.

Different solvent configurations exhibit distinct interactions related to their polarity and dielectric constant. Reported ether solvents can be categorized into three groups according to their structures: linear ethers, cyclic ethers and fluoro-ether, such as DME, DEGDME, TEGDME and DEE, contain more than two ether–oxygen bonds of chelating coordination with Na$^+$, providing strong sodium salt solubility and can be applied alone as the main solvent. Cyclic ethers, such as THF, DOL and MTHF, contain one or two ether–oxygens, and exhibit slightly weaker solvation ability compared to linear ethers, making them ideal co-solvents when paired with linear ethers. Fluoro-ethers (HFME, BTFE, TFEE) possess a higher content of fluorine with
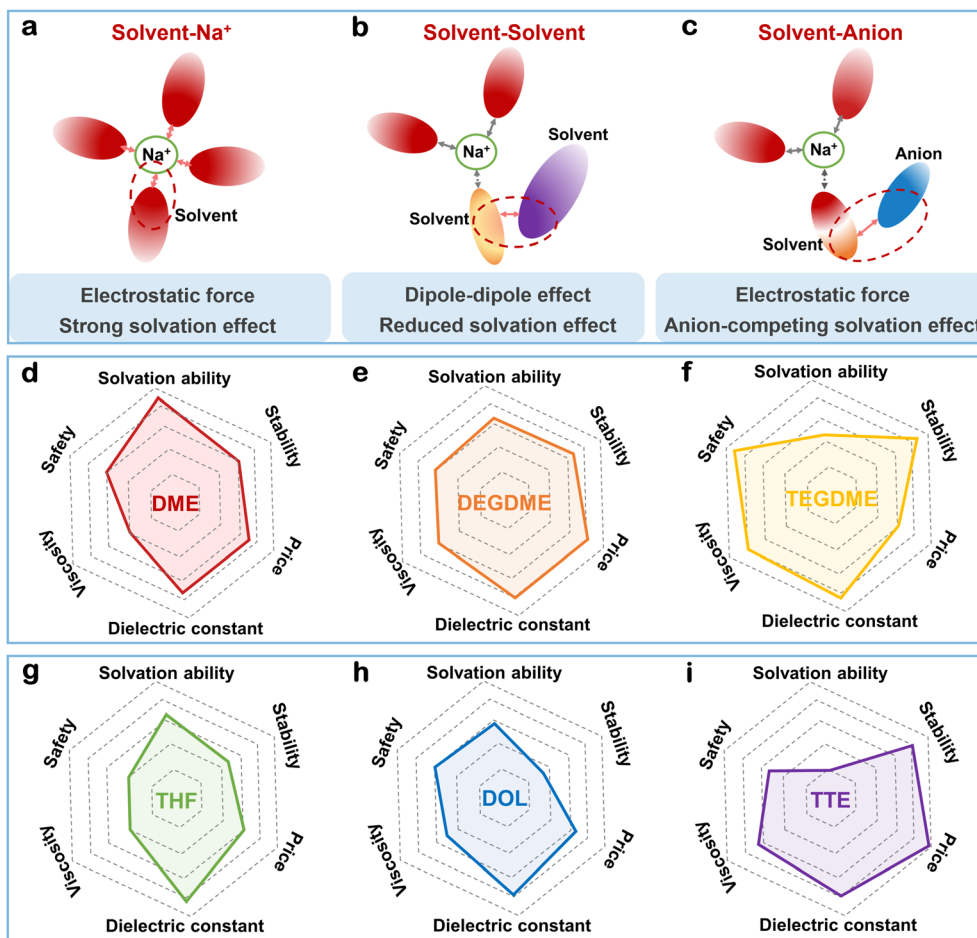
6880 | Energy Environ. Sci., 2025, 18, 6874–6898

This journal is © The Royal Society of Chemistry 2025

Fig. 5 Solvation effects and key properties of ethers. Solvation effect of (a) solvent−Na$^+$, (b) solvent−solvent and (c) solvent−anion. (d)−(i) Overview of key properties of ethers.

electron-absorbing properties,[92,105,106] resulting in low Na$^+$ solvation capabilities and poor sodium salt dissolution. Therefore, fluoro-ethers are generally used as diluents.

The properties of ethers, including solvation ability, stability, safety, viscosity, dielectric constant and price, are summarized in Fig. 5(d)–(i). Linear ethers and cyclic ethers excel in terms of solvation ability, dielectric constant, viscosity and affordability, while fluoro-ethers offer superior antioxidant stability. However, the high cost of fluoro-ethers, attributed to their complex manufacturing process,[107] poses a challenge for their large-scale commercial application. It is worth noticing that TEGDME stands out for its exceptional safety,[108] as demonstrated by its high flash, boiling point, and non-flammability. These properties position TEGDME as a highly promising candidate for commercialization.

Ether can be applied independently as an electrolyte solvent, in a mixture of more than two ethers, or as a diluent. Representative formulations of ether-based electrolytes for SIBs are summarized in Fig. 6, along with the corresponding cathodes and anodes. From top to bottom are linear ether, cyclic ether and fluorinated ether. Linear ether is mostly used alone due to its high solubility and moderate solvation ability, and is typically paired with HC or sodium metal anodes, and polyanionic

and layered oxide cathodes. Research indicates that HC in linear ether demonstrates excellent rate performances and low-temperature performances, with discharge capacities significantly higher than those in ester-based electrolyte at large current density and low temperature, resulting in its kinetic advantage.[109] When linear ethers are matched with high-voltage cathodes, co-salts such as NaBF$_4$ are often added to derivatize a stable CEI to enhance the high-voltage stability.[110]

Some cyclic ethers with lower solubility, such as MTHF, DOL, *etc.*, are often mixed with linear ethers with high solubility. The cathodes and anodes applied in these systems are similar to those of linear ethers. Fluorinated ethers, which show poor solubility for sodium salts, are used as diluents to shield the electrostatic interaction between solvent–Na$^+$, coulombic interaction between anion–Na$^+$, and the dipole interaction between solvent–solvent in highly concentrated salt systems. This enhances the reversibility and durability of the sodium-metal batteries in low-temperature environments, which is crucial for cold-climate applications. NaPF$_6$, sodium trifluoromethanesulfonate (NaOTf), sodium bis(trifluoromethylsulfonyl)imide (NaTFSI) and sodium bis(fluorosulfonyl)imide (NaFSI) were used as the primary salts,[129] while NaBF$_4$ was used

This journal is © The Royal Society of Chemistry 2025

Energy Environ. Sci., 2025, **18**, 6874–6898 | **6881**

Solvent type		Cathode	Electrolyte composition	Anode	Ref
Linear ether Main solvent	High	Hard carbon	1 M NaPF$_6$ in DME	Na	113
		Hard carbon	0.5 M NaPF$_6$ in DEGDME	Na	114
		Hard carbon	1 M NaPF$_6$ in DEGDME	Na	115
		Hard carbon	1 M NaOTf in DEGDME	Na	57
		Graphite	1 M NaPF$_6$ in DEGDME	Na	116
		Hard carbon	1 M NaPF$_6$ in TEGDME	Na	117
Linear ether Main solvent High voltage	Solubility	Na$_3$V$_2$(PO$_4$)$_3$	0.5 M NaPF$_6$ in DEE	Na	118
		Na$_3$(VOPO$_4$)$_2$F@rGO	1 M NaPF$_6$ in DEGDME	Na	111
		Na$_3$V$_2$(PO$_4$)$_3$	0.6 M NaOTf + 0.4 M NaBF$_4$ in DEGDME	p-Al@C	119
		NaNi$_{1/3}$Fe$_{1/3}$Mn$_{1/3}$O$_2$	0.9 M NaPF$_6$ + 0.1 M NaBF$_4$ in TEGDME	Hard carbon	120
		Na$_3$V$_2$(PO$_4$)$_3$	1 M NaPF$_6$ in DEGDME + [C$_4$C$_1$im][BF$_4$]	Na	121
Cyclic ether Co-solvent		Hard carbon	1 M NaPF$_6$ in THF + MTHF	Na	122
		Na$_3$V$_2$(PO$_4$)$_3$	0.5 M NaOTf in DOL + DEGDME	Na	66
		Na$_3$V$_2$(PO$_4$)$_3$	1 M NaPF$_6$ in DOL + DEGDME	Cu	123
		Prussian blue	1 M NaPF$_6$ in THF + PC	Hard carbon	124
		Na$_{0.44}$MnO$_2$	1 M NaPF$_6$ in MTHF + DEGDME	Na	125
		Na$_3$V$_2$(PO$_4$)$_2$O$_2$F	3.04 M NaPF$_6$ in DOL + DEGDME	Hard carbon	65
Fluoro-ether Diluent	Low	Na$_{0.67}$MnO$_2$	NaFSI in HFME + DEGDME	Na	112
		Na$_3$V$_2$(PO$_4$)$_3$	NaTFSI in TFEE + [Py$_{13}$][FSI]	Na	126
		Na$_3$V$_2$(PO$_4$)$_3$	NaFSI in BTFE + DME	Na	62
		Na$_3$V$_2$(PO$_4$)$_3$	NaFSI in OTE + DME	Na	75
		NaCu$_{1/9}$Ni$_{2/9}$Fe$_{1/3}$Mn$_{1/3}$O$_2$	NaFSI in TTE + TEP	Hard carbon	127
		Na$_{0.95}$Ni$_{0.4}$Fe$_{0.15}$Mn$_{0.3}$Ti$_{0.15}$O$_2$	NaPF$_6$ + NaDFOB in TTE + TMP	Na	128

Fig. 6 Ether-based electrolyte composition and matching cathodes and anodes in sodium batteries.[57,62,65,66,75,111–128]

as the secondary salt due to its low solubility. Among them, NaPF$_6$ is the most commercially viable salt due to its advantages in film formation, low cost, and non-corrosiveness to aluminum foil.[130–132] In the past years, electrolyte design has mainly focused on regulating the solvation structure of Na$^+$, as this not only affects Na$^+$ transport but also alters the composition of the interphase. Recently, the solvation structure involving anions has attracted some attention, which also affects the formation of the interphase and the desolvation energy barrier of Na$^+$. However, the anion–solvent interactions, even in the simplest single-salt, single-solvent electrolyte systems, are still not yet fully understood. Future studies, deeply exploring the mechanism of anion solvation structure will provide new directions for optimizing electrolyte design.

Ether-based electrolytes generally outperform ester-based electrolytes in terms of ICE, rate and low-temperature performance when paired with HC and Na metal. Specifically, in ether-based electrolyte (1 M NaOTf in DEGDME),[57] HC achieves an ICE of up to 91.2% with superior high-rate capability, ultralong cycle life (93% capacity retention over 1000 cycles at 200 mA g^{-1}) and outstanding low-temperature performance. Studies reveal that the lower electrochemical reaction kinetics can be significantly improved in ether-based electrolytes. For instance, Yang et al. overcome salt precipitation at temperatures far above the freezing point of solvents by tuning the entropy of solvation in a strong solvation and weak solvation solvent mixture. This enables the solvation structure to

spontaneously transform at low temperature to avoid salt precipitation, endowing a temperature-adaptive feature to the electrolyte.[68] This temperature-adaptive electrolyte exhibited an excellent low-temperature performance in a Na$_{2/3}$Ni$_{1/4}$Cu$_{1/12}$-Mn$_{2/3}$O$_2$/HC full cell with 90.6% capacity retention over 400 cycles at −40 °C. Zheng et al. reported that by using a hydrofluoroether as an "inert" diluent, the salt concentration could be significantly reduced ($\leq$1.5 M),[62] while maintaining the solvation structures of high concentration electrolytes. This formed a localized high concentration electrolyte (2.1 M NaFSI in DME/BTFE), enabling dendrite-free Na deposition with a high coulombic efficiency of >99%, fast charging (20C) and stable cycling (90.8% retention after 40 000 cycles) in Na$_3$V$_2$(PO$_4$)$_3$/Na batteries.

Polyanionic and layered oxide cathodes, which have a charging cut-off voltage of around 4.0 V, obtain satisfactory cycling stability in ether-based electrolytes. Using 1 M NaPF$_6$ in DEGDME as the optimized ether-based electrolyte, a robust fluorine-rich inorganic–organic interphase was identified, which effectively ameliorates the interface, facilitates ultrafast charge transfer and stabilizes high-voltage cathodes over 10 000 times with the help of cathode engineering.[111] Similarly, a weakly coordinating diluent, HFME, was applied to regulate the coordination of Na$^+$ with DEGDME and anion, forming a diluent-participated solvate.[112] This unique solvation structure promotes the accelerated decomposition of anions and diluents, leading to the construction of robust inorganic-rich electrode–electrolyte interphases. As a

result, the $Na_{0.67}MnO_2$/Na cell delivered a high-capacity retention of 87.3% with a high average coulombic efficiency of 99.7% after 350 cycles.

Briefly, the ether-based electrolyte exhibited good compatibility with both anodes and cathodes of SIBs. Nevertheless, the electrolyte is a complex solution system, where intertwined interactions between ion–ion, ion–solvent, and solvent–solvent jointly affect the thermodynamic and kinetic processes. Different cathodes and anodes have distinct electrolyte requirements, and it is crucial to analyze the role of electrolytes in relation to specific electrode materials. This in-depth analysis will further promote our understanding of the modification mechanism of ether-based electrolytes in SIBs.

5. Critical effects of ether in anodes and cathodes of SIBs

Ether-based electrolyte, in addition to serving as a medium for ion migration and enabling ion conduction between the cathode and anode, plays a significant role in a battery's energy density, cycle life, rate performance and low-temperature performance, etc., which is reflected through the interaction with cathode and anode materials. This section highlights the decisive effects of ether-based electrolytes in specific cathode and anode materials.

5.1 Ether-based electrolytes for anodes

The high suitability of ether-based electrolytes for sodium batteries is mainly reflected in their favorable interactions with HC and Na metal anodes. The electrochemical performance of ether in HC/Na and Na/Na cells was evaluated and shown in Fig. 7(a). Obviously, the rate performance of HC in the ether-based electrolyte (1 M $NaPF_6$ in DEGDME) significantly outperforms that of the ester-based electrolyte (1 M $NaPF_6$ in EC/DMC), especially at current densities higher than 0.2 A g^{-1}. For the Na/Na cell, the polarization voltage with the ether-based electrolyte (1 M $NaPF_6$ in DEGDME) is significantly smaller than that of the ester-based electrolyte (1 M $NaPF_6$ in EC/DMC). The above comparison fully illustrates the kinetic advantage of ether-based electrolytes on HC and Na metal.

HC, recognized as the most promising anode material for commercial application, exhibits unique properties that make it well-suited for SIBs. Its rich microcrystalline structure facilitates Na^+ absorption, embedding and de-embedding, resulting in a high specific capacity (300–350 mA h g^{-1}) and a low operating potential (~0.1 V vs. Na/Na^+).[133–135] However, its large specific surface area, compared with that of the graphite, increases electrolyte consumption to construct SEI, making interfacial stability highly dependent on the electrolyte. Additionally, the larger layer spacing in HC provides a higher possibility of solvent and Na^+ co-embedding in the HC layer, with the impact of this behavior depending on the solvent's solvation capacity and reduction stability. Research suggests that the cyclic ethers have a weaker solvation ability than the cyclic ester, resulting in lower desolvation energy.[52,122]

The LUMO energy level is a critical indicator reflecting the stability of solvent reduction.[136] As shown in Fig. 7(b), the energy difference between the Fermi energy level of the anode and the LUMO energy level of the electrolyte determines the thermodynamic stability of the electrolyte at the anode and the formation of SEI films. More specifically, if the LUMO energy level of the electrolyte is lower than the Fermi energy level of the anode, the electrolyte will accept electrons from the anode and initiate a reduction reaction. Ethers, with higher LUMO energy levels than that of esters, exhibit better stability with low-potential anodes. Compared to esters, ethers display superior kinetic compatibility with HC, and it is evident that sodium batteries using ether-based electrolytes exhibit superior rate and low temperature performance compared to ester-based electrolytes (Table 2). Several possible factors may contribute to this advantageous situation, including thin SEI, high Na^+ diffusion coefficients, and reversible co-intercalation of ether–Na^+ (Fig. 7(c)).

Na-metal anodes, with their high theoretical capacity (1166 mA h g^{-1}) and low redox potential (−2.71 V, vs. SHE), are expected to realize high energy density energy storage.[140–142] Currently, the energy density of sodium–metal batteries reported in the literature is substantially higher than those of SIBs, up to 200~300 W h kg^{-1}.[143,144] However, the Na-metal anode faces many challenges during cycling,[145,146] such as inhomogeneous Na deposition and severe Na dendritic growth, unstable SEI, and drastic volumetric fluctuations arising from the repetitive depositing/stripping process. Highly chemically active Na metal reacts spontaneously with the electrolyte to form a loose and fragile passivation film, which is difficult to withstand the volume expansion and stress during Na deposition, leading to its rupture.[147] The cracks may become active sites for the growth of Na dendrites, contributing to the rapid formation of Na dendrites, thus seriously affecting the electrochemical performance of Na metal batteries and hindering their practical applications.[148] Compared to the esters, ethers demonstrate superior interfacial compatibility with Na metal, forming homogeneous and thin SEI, and the moderate ether–Na^+ solvation structure derived from the ether-based electrolyte (Fig. 6(c)). These features help suppress dendrite growth and enhance cycling stability.

HC anodes in ether-based electrolytes exhibit higher initial coulombic efficiencies, better rate performances and low-temperature performances compared to conventional ester electrolytes. However, the mechanism behind the faster Na storage kinetics for HC in ether-based electrolytes remains a topic of ongoing debate. One proposed explanation is the formation of a thin dual-SEI model[149] (Fig. 8(a)) derived from the ether-based electrolyte, consisting of an I-SEI (the SEI inside the nanopore) and S-SEI (the SEI formed on the surface). The S-SEI formed in the ether electrolyte (1 M $NaPF_6$ in DEGDME) is very thin and even negligible due to the excellent reductive stability of ethers (Fig. 8(b)). In contrast, the S-SEI formed in the ester-based electrolyte (1 M $NaPF_6$ in EC/DEC) is significantly thicker, reaching about 10 nm (Fig. 8(c)) after 10 cycles. The I-SEI can be detected by small-angle X-ray scattering (SAXS), and

This journal is © The Royal Society of Chemistry 2025

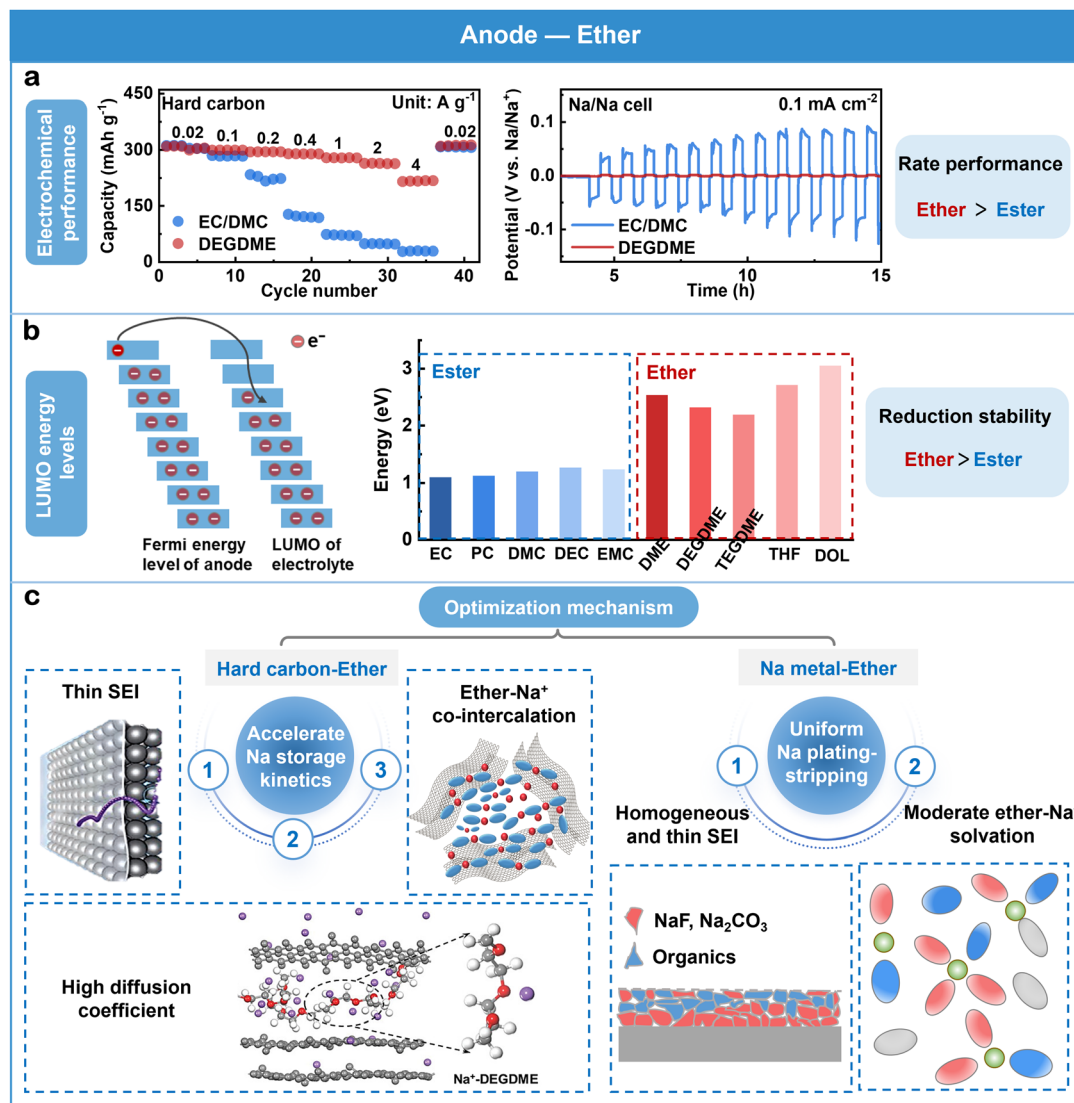Energy Environ. Sci., 2025, **18**, 6874–6898 | **6883**

Fig. 7 Critical effects of ether in the anodes of sodium batteries. (a) Electrochemical performance. (b) LUMO energy levels of esters and ethers. (c) Optimization mechanism of ether on HC and Na metal anodes.

Table 2 Rate and low-temperature performance of batteries using different ether-based electrolytes

Solvent	Electrolyte	Electrode	Performance	Ref.
DME	1 M NaPF$_6$ in DME	Hard carbon/Na	>240 mA h g^{-1} at 10C	113
		NaNi$_{0.5}$Mn$_{0.5}$O$_2$/Na	102.7 mA h g^{-1} at 10C	137
DEGDME	0.5 M NaPF$_6$ in DEGDME	Hard carbon/Na	310 mA h g^{-1} at −30 °C	114
	1 M NaPF$_6$ in DEGDME	Hard carbon/Na	161 mA h g^{-1} at 4 A g^{-1}	115
	0.6 M NaOTf + 0.4 M NaBF$_4$ in DEGDME	Na$_3$V$_2$(PO$_4$)$_3$/p-Al@C	67 mA h g^{-1} at −40 °C	119
TEGDME	1 M NaPF$_6$ in TEGDME	Hard carbon/Na	>180 mA h g^{-1} at 2C	117
THF	1 M NaPF$_6$ in THF	Hard carbon/Na	212 mA h g^{-1} at 5 A g^{-1} and 175 mA h g^{-1} at −20 °C	138
	1 M NaPF$_6$ in PC/THF	Prussian blue/hard carbon	65.6 mA h g^{-1} at 5C	124
	1 M NaPF$_6$ in THF/MTHF	Na$_3$V$_2$(PO$_4$)$_3$/hard carbon	61.4 mA h g^{-1} at −40 °C	122
MTHF	0.8 M NaPF$_6$ in MTHF	Na$_3$V$_2$(PO$_4$)$_3$/Al@C	>70 mA h g^{-1} at −40 °C	139
DOL	0.5 M NaOTf in DEGDME/DOL	Na$_3$V$_2$(PO$_4$)$_3$/Na	68 mA h g^{-1} at −40 °C	66
	0.4 M NaPF$_6$ in DEGDME/DOL	Na$_3$V$_2$(PO$_4$)$_3$/Al@C	59.7 mA h g^{-1} at −40 °C	123
OTE	NaFSI : OTE : DME = 1 : 1.5 : 3 (molar ratio)	Na$_3$V$_2$(PO$_4$)$_3$/Na	79.9 mA h g^{-1} at 24C	75
Esters	1 M NaPF$_6$ in EC/DMC	Hard carbon/Na	<50 mA h g^{-1} at 10C	113
	1 M NaClO$_4$ in EC/DEC + 5 vol% FEC	NaNi$_{0.5}$Mn$_{0.5}$O$_2$/Na	78.5 mA h g^{-1} at 10C	137
	1 M NaPF$_6$ in PC	Prussian blue/hard carbon	26.9 mA h g^{-1} at 5C	124

6884 | *Energy Environ. Sci.*, 2025, **18**, 6874–6898

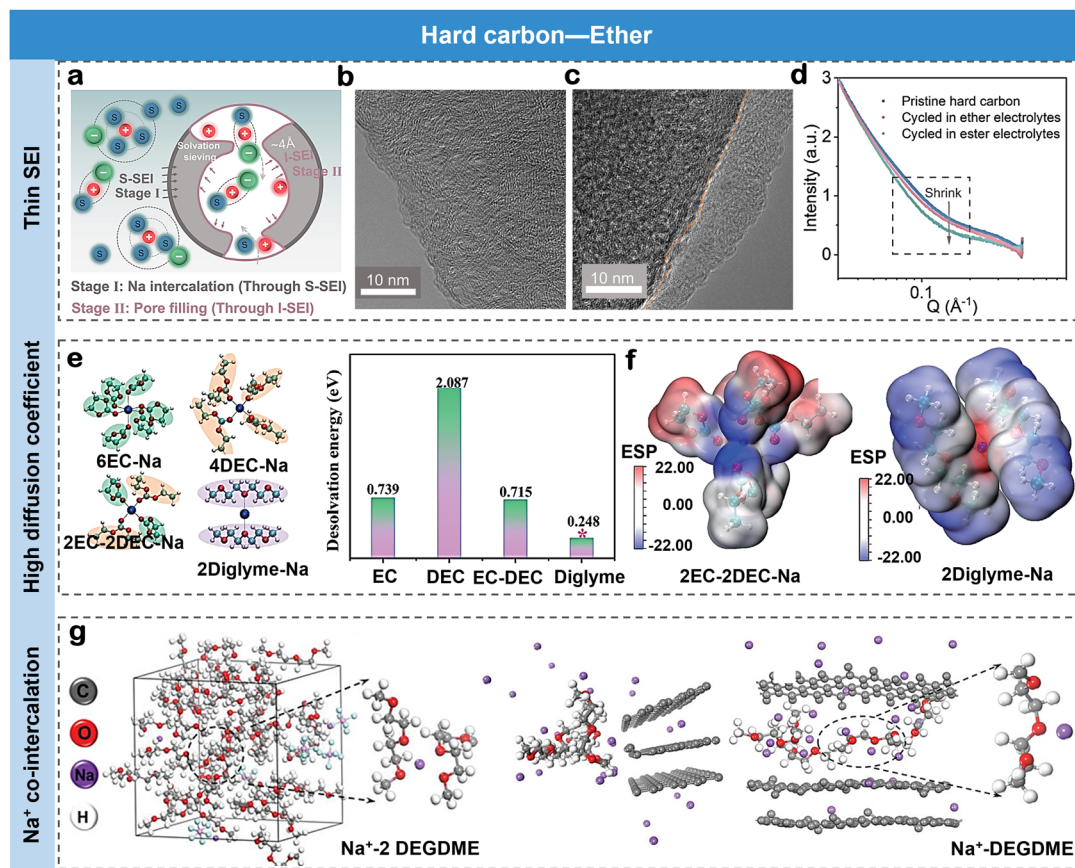This journal is © The Royal Society of Chemistry 2025

Fig. 8 Analysis of the critical role of ether in the HC of sodium batteries. (a)–(d) Thin SEI. Reproduced with permission,[149] Copyright © 2024, The Authors. (e) and (f) High Na^{+} diffusion coefficient. Reproduced with permission,[150] Copyright © 2023, Tsinghua University Press. (g) Ether–Na^{+} co-intercalation. Reproduced with permission,[64] Copyright © 2021 Wiley-VCH GmbH.

also shows differences in the pore volume shrinkage in HC with both electrolytes after cycling (Fig. 8(d)). However, the shrinking of the pore volume is more severe in the ester-based electrolyte, indicating that a thicker SEI is formed within the nanopores. This finding further underscores the superior performance of the ether-based electrolyte in stabilizing the SEI and enabling efficient Na storage.

The enhanced rate performance demonstrated by HC in ether-based electrolytes is attributed to a high Na^{+} diffusion coefficient (Fig. 8(e) and (f)).[150] Molecular dynamics (MD) simulation reveals that the diffusion coefficient of Na^{+} ions in the ether-based electrolyte (1 M NaPF$_6$ in DEGDME) is about 2.5 times higher than that in the ester-based electrolyte (1 M NaPF$_6$ in EC/DEC) when Na^{+} ions are diffused in the electrolyte. When the solvated Na^{+} ions diffused into the SEI interface and the HC, the enhanced charge transfer kinetics (low R_{SEI} (1.5 vs. 24 Ω)) at the SEI, combined with low desolvation energy (0.248 eV), contribute to high-rate performance and good cycling stability of HC in the ether-based electrolyte.

The solvated Na^{+} was calculated by the mean square displacement (MSD).[64] The calculated diffusion coefficients of solvated Na^{+} in the ether-based electrolyte (1 M NaPF$_6$ in DEGDME) and ester-based electrolyte (1 M NaPF$_6$ in EC/DEC) are 1.21×10^{-6} and 8.88×10^{-7} cm^2 s^{-1}, respectively, indicating

faster solvated Na^{+} diffusion kinetics in the ether-based electrolyte. The final structure of the Na^{+}-DEGDME interaction and its intercalation into the carbon layers is shown in Fig. 8(g). The interlayer spacing increased from 4 to ≈ 9 Å after the intercalation of four Na^{+}-DEGDME. The final configurations indicate that the Na^{+} and ether–Na^{+} co-intercalation in the ether-based electrolyte mitigates the sluggish desolvation process, thus enhancing the kinetics.

Based on existing research, the accelerated Na storage kinetics in ether-based electrolytes can be attributed to three key factors: thin SEI, high Na^{+} diffusion coefficient, and ether–Na^{+} co-intercalation. These findings offer valuable insights for the development of other high kinetics electrolytes.

The compatibility of ether-based electrolytes with Na metal is mainly demonstrated by high coulombic efficiency and long cycle life, achieved by uniform Na depositing/stripping. This performance is critically dependent on a uniform and thin SEI and a moderate Na^{+}–ether solvation structure.[151] The representative ester-based electrolyte of 1 M NaPF$_6$-PC and ether-based electrolyte of 1 M NaPF$_6$-DEGDME in Na/Cu cells are shown in Fig. 9(a). Obviously, in 1 M NaPF$_6$-PC, Na/Cu cells present very low coulombic efficiency (less than 20%), demonstrating poor Na deposition reversibility. In sharp contrast, the average coulombic efficiency of Na/Cu cell cycled in 1 M NaPF$_6$-diglyme
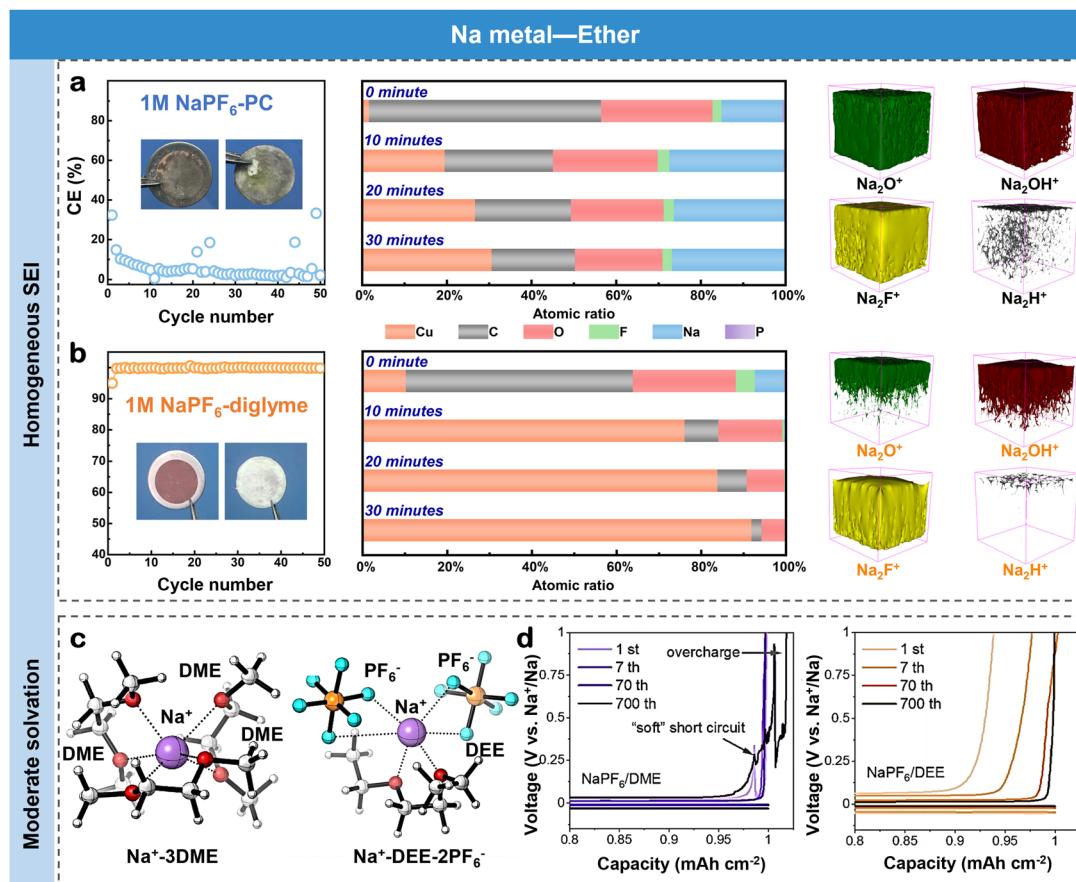
Fig. 9 Analysis of the critical role of ether in Na metal of sodium batteries. (a) and (b) Homogeneous SEI. Reproduced with permission,[151] Copyright © 2023 Elsevier B.V. (c) and (d) Moderate solvation. Reproduced with permission,[153] Copyright © 2023 Wiley-VCH GmbH.

is close to 100% (Fig. 9(b)). Large amounts of NaH are distributed across the surface and bulk body of "dead deposits" when cycled in 1 M NaPF$_6$-PC, while only a small amount of NaH is observed at the surface of "dead deposits" when cycled in 1 M NaPF$_6$-diglyme. Significantly, Kim *et al.* reported that[152] compared to fluorine-containing ester-based electrolyte (1 M NaClO$_4$ in EC/PC + 5 wt% FEC), an ether-based electrolyte (1 M NaBH4 in DEGDME) facilitated the formation of NaH, which is considered a favorable SEI component due to its excellent mechanical properties and electronic insulation. Specifically, the native oxide surface of sodium was converted into NaH and NaBO$_2$ after soaking in the electrolytes, implying that "SEI reconstruction" occurred by chemical reduction. Accordingly, the Na/Na symmetric cell exhibited significantly extended cycling stability (1200 h, 1 mA cm^{-2}, 1 mA h cm^{-2}) compared to the fluorine-containing ester-based electrolyte (300 h for 1 M NaClO4 in EC/PC + 5wt% FEC). However, the precise quantity and formation mechanism of NaH, as well as its impact on cell performance, remain to be elucidated.

MD simulations were utilized to investigate the solvation structures of Na$^+$.[153] Due to the strong chelation capacity of the DME solvent, 95% solvent-surrounded Na$^+$ is present in 0.5 M NaPF$_6$/DME electrolyte (Fig. 9(c)). Comparatively, the solvent-surrounded Na$^+$ solvation sheath occupies a low proportion of

25% in 0.5 M NaPF$_6$/DEE electrolyte. In this case, the Na$^+$ anion single pairs and Na$^+$ anion clusters with coordinated PF$_6^-$ anion account for 35% and 40%, respectively, demonstrating the anion-involved solvation structure is dominant. The voltage-capacity profiles for NaPF$_6$/DEE electrolyte demonstrate stable plating/stripping behavior (Fig. 9(d)), while NaPF$_6$/DME electrolyte shows abnormal voltage fluctuations and overcharging appeared, illustrating the presence of the "soft" short circuit. These results demonstrate that weak solvation structure with anionic participation contributes to the cycling stability of Na metal.

Recent reports have also highlighted the absence of a SEI on co-intercalated HC when ether-based electrolytes are used. Therefore, it is crucial to understand the exact correlation of SEI with different carbon microstructures for the rational design of specific electrolytes tailored for specific HC anodes. For the Na metal anode, ether-based electrolytes can facilitate the formation of a stable SEI and moderate solvation, which can largely reduce polarization and facilitate fast Na$^+$ diffusion. Although it is well known that apparent volume expansion and phase change occur during the electrochemical reaction of metal-based anodes, high reversibility can still be obtained with ether-derived interphase over prolonged cycling. Therefore, it is insufficient to solely investigate the final microstructure and

6886 | *Energy Environ. Sci.*, 2025, **18**, 6874–6898

This journal is © The Royal Society of Chemistry 2025

composition of SEI after dynamic changes in the solvation. This underscores the need for *in situ* characterization to monitor how ether-derived SEI forms and how its microstructure and composition evolve during charging and discharging

5.2 Ether-based electrolytes for cathodes

The mainstream cathodes for SIBs include layered oxides, Prussian blue compounds, and polyanionic compounds. Layered oxides are the preferred cathode because of their facile preparation method and high energy density. However, the high charging state of layered oxides can catalyze electrolyte decomposition and trigger interfacial parasitic reaction, which affects cycle performance and safety of batteries.[154,155]

Prussian blue compounds offer advantages such as high energy density and adjustable operating voltage, however, the presence of water in the lattice compromises the long-term stability of the electrolyte.[156,157] Polyanionic compounds, on the other hand, are known for their excellent stability and high operating voltage, but suffer from low conductivity, which limits their rate and low-temperature performance.[158,159] The upper voltage window of the above cathodes is typically $\geqslant 4.0$ V, thereby placing high demands on the oxidative stability of the electrolyte. The suitability of ether-based electrolytes in high-voltage applications has been questioned. For example, early studies in LIBs highlighted that ether-based electrolytes are incompatible with $LiCoO_2$ cathodes, which are typically charged above 4.0 V to provide more capacity. The lone pairs of electrons on oxygen atoms of ether molecules make them susceptible to electrophilic attack, resulting in low oxidative stability. Two strategies have been proposed to enhance the upper electrochemical stability window of the electrolyte:[160] (i) thermodynamically enhancing the intrinsic electrochemical window, and (ii) kinetically constructing a stable CEI to slow down the electrolyte decomposition.

In Fig. 10(a), the energy difference between the Fermi energy level of the cathode and the HOMO energy level of the electrolyte determines the thermodynamic stability of the electrolyte at the cathode, influencing the possibility for the formation of the CEI film.[32,136] More specifically, if the HOMO energy level of the electrolyte is higher than the Fermi energy level at the cathode, the electrolyte will lose electrons, triggering oxidation and decomposition. The ether-based electrolyte with a high HOMO energy level fails to thermodynamically offer high-voltage stability, as a result, they are often optimized from a kinetic perspective to form a robust CEI at the cathode. As shown in Fig. 10(b), the CEI generated from ether-based electrolyte can raise the electrochemical stability window to accommodate the required high-voltage of cathodes. The compositions and structures of the CEI play a critical role in modifying the electrochemical properties of SIBs, such as rate performance, cycle life, and high/low-temperature performance.

Most current studies on the high-voltage performance of ether-based electrolytes focus on functional additives and solvated structures (Fig. 10(c)),[161,162] and the upper voltage window reported in the literature is in the range of 4.0–4.5 V. Corresponding cathodes and upper voltage windows are summarized

in Table 3. Introducing functional additives to build a robust inorganic-rich CEI can effectively inhibit the decomposition of ethers at the interface. Common additives include fluorinated ethylene carbonate (FEC),[142] sodium difluoro-oxalate borate (NaDFOB),[163] and sodium difluorophosphate (NaDFP),[164] among others. The solvation structure of ether-based electrolytes can be adjusted by modulating both sodium salt and solvent.[165,166] Adjusting the concentration and type of sodium salts reduces the proportion of free ether solvent, thereby constructing a stable CEI primarily composed by the sodium salts decomposition products.[65,167] Additionally, altering the solvent structure, such as the introduction of electron-absorbing groups, can strengthen the solvated structure, improving the oxidative stability of the electrolyte.[168] Although incorporating fluorine substituent groups into the structure of ether molecules can improve the oxidative stability, this strategy greatly increases the cost of electrolytes, making it not suitable for large-scale applications.

The research on electrolytes must be closely linked to the cathode materials with which they interact. The CEI is essential to prevent irreversible reactions between the cathode and the electrolyte, maintaining the lattice structure of the cathode, and inhibiting the dissolution of active materials. By refining the volume ratio of two conventional linear ether solvents, a binary electrolyte[172] (1 M $NaPF_6$ in DEGDME/TEGDME) can form a cation solvation structure that is well-adaptive for high-voltage Na (de)intercalation of P2-/O3-type layered oxide cathodes. Anode-free batteries using this optimized electrolyte have demonstrated high coulombic efficiency, extended cycle life, and a cell-level specific energy density exceeding 300 W h kg^{-1} (Fig. 11(a)). This performance is attributed to the NaF- and Na_2CO_3-rich interphase generated from the CO_2-regulated solvated structure of the binary electrolyte (Fig. 11(b)).

A weakly solvating anion-stabilized electrolyte, which balances the interaction between the Na$^+$–solvent and Na$^+$–anion, is proposed to optimize the electrochemical performance of $NaNi_{1/3}Fe_{1/3}Mn_{1/3}O_2$ (NFM) cathodes.[167] In Fig. 11(c), the HOMO energy level of different solvated clusters is calculated using density functional theory (DFT) to analyze the oxidative tendency. More specifically, the HOMO energy levels of Na$^+$–DME–PF$_6^-$ and Na$^+$–DME–2PF$_6^-$ were −8.39 eV and −5.21 eV, respectively, indicating that increasing PF$_6^-$ in the solvated cluster raises the HOMO level. Meanwhile, to verify the outstanding performance of weakly solvating anion-stabilized electrolyte, the industrial anode-free pouch cells were constructed under harsh conditions. These cells exhibit a high capacity of 180 mA h, a lean electrolyte ratio of 4 g A h^{-1}, and a multi-layer structure, maintaining more than 80% of their initial capacity after 50 cycles (Fig. 11(d)). In addition, the low-temperature performance of the Cu||NFM pouch cell was assessed after charging at room temperature, and these cells delivered 95.5%, 91.6%, 87.2%, 78.4%, and 74.3% of their room temperature capacity at temperatures of 10 °C, 0 °C, −10 °C, −20 °C, and −30 °C, respectively. These results further demonstrate the superior low-temperature applicability of the electrolytes (Fig. 11(e)). Wang *et al.* successfully passivated the reactive sites of terminal H on DEGDME solvents, inhibiting further dehydrogenation and
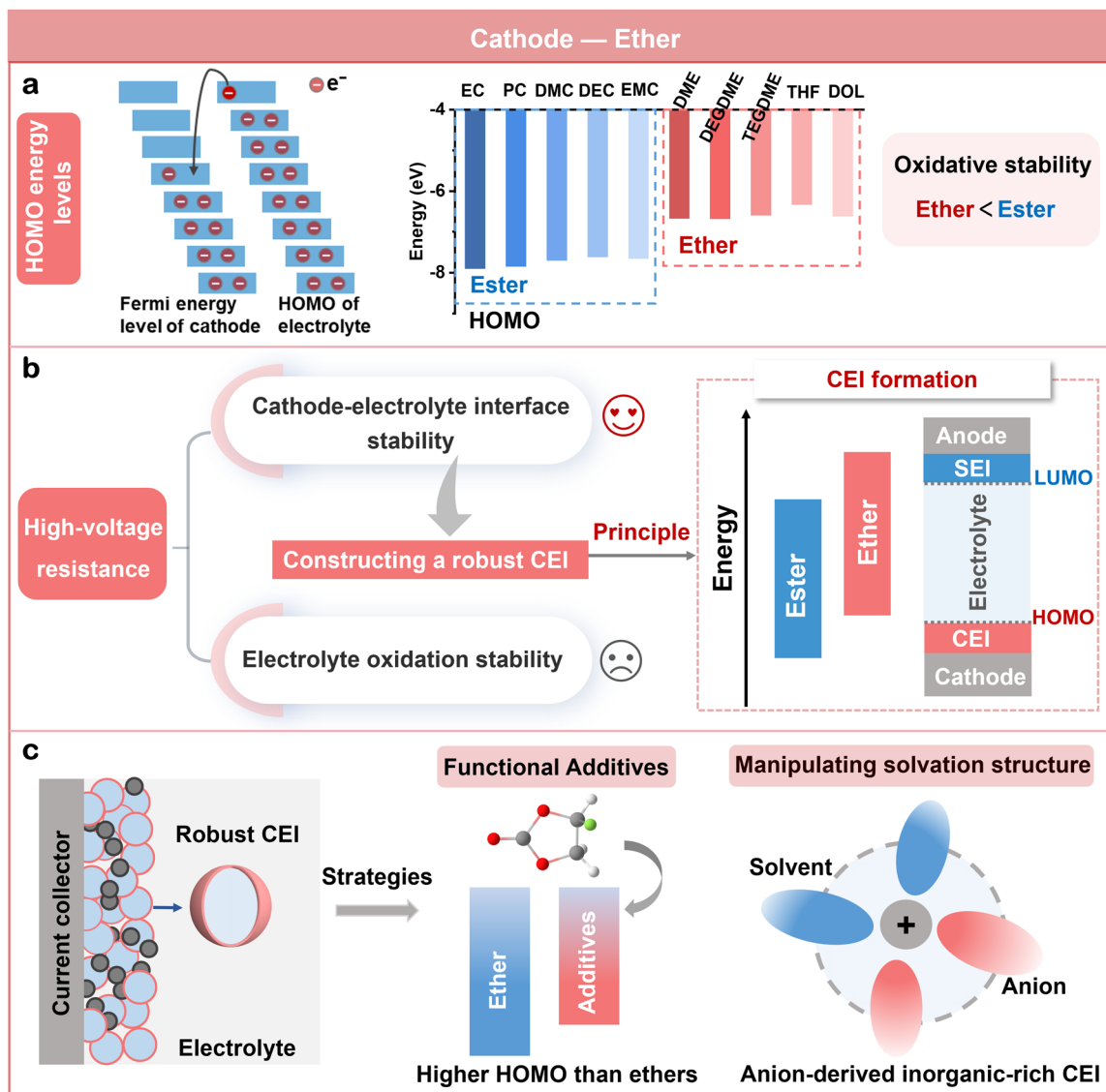
This journal is © The Royal Society of Chemistry 2025

Energy Environ. Sci., 2025, **18**, 6874–6898 | **6887**

Fig. 10 Critical effects of ethers in the cathodes of sodium batteries. (a) HOMO energy levels of esters and ethers. (b) Optimization mechanism of ethers on cathodes. (c) Strategies for forming a robust CEI.

oxidation during battery operation, by introducing a small amount of nitrate anions (NO_3^-) into the DEGDME-based electrolyte (Fig. 11(f)–(h)). The electron-donating ability of NO_3^- weakened the Na^+–solvent interactions, promoting the decomposition of OTf^- and NO_3^- anions, leading to the formation of a robust CEI. This CEI, rich in NaF and NaN_xO_y components, demonstrated enhanced tolerance to high voltages.[175]

As demonstrated by Wu et al.,[65] the fully coordinated ether-based electrolyte with strong resistance against oxidation is rationally designed for solvation configuration. This electrolyte remains anodically stable when paired with a high-voltage $Na_3V_2(PO_4)_2O_2F$ (NVPF) cathode under 4.5 V (vs. Na/Na^+), which may be contributed by effective protection of the CEI. The assembled graphite//NVPF full cells exhibit superior rate performance and unprecedented cycling stability (Fig. 12(a)–(c)). Fig. 12(d) provides the proportions of typical micro-structures

within the primary solvation sheath.[170] It is found that Na^+ in G1 (1 M $NaPF_6$ in DME) and G2 (1 M $NaPF_6$ in DEGDME) electrolytes are chiefly surrounded by solvent molecules, with a high proportion of 99.92% and 99.80%, respectively. In DEE (1 M $NaPF_6$ in DEE) and G4 (1 M $NaPF_6$ in TEGDME) electrolytes, structures containing PF_6^- anions account for 59.59% and 16.77%, respectively. Associated with the electrochemical behaviors of different electrolytes, it can be rationally speculated that it is the anion-dominated solvation structure that motivates the deficient high-voltage stability of G4, especially the DEE electrolyte. This implies that the strong solvation structure without anion participation is more suitable for high-voltage sodium batteries. However, this conclusion appears to contradict the findings shown in Fig. 9(c), (d) and 11(c)–(e). And this apparent contradiction arises from the lack of absolute parameters to quantify the solvated structure. Although parameters such as the

6888 | Energy Environ. Sci., 2025, **18**, 6874–6898

This journal is © The Royal Society of Chemistry 2025

Table 3 The upper voltage windows of batteries using different ether-based electrolytes

Electrolyte	Cathode	Upper voltage	Ref.
NaFSI : DEGDME : DM = 1 : 1.4 : 5.3 (molar ratio), (N-dimethyltrifluoro-methanesulfonamide)	$NaNi_{1/3}Fe_{1/3}Mn_{1/3}O_2$	4.2 V	169
1 M $NaPF_6$ in DEGDME	$Na_3(VOPO_4)_2F$	4.3 V	170
0.03 M $NaBF_4$ (additive) + 0.3 M $NaPF_6$ in DEGDME	$Na_3(VOPO_4)_2F$	4.3 V	171
NaTFSI : TFEE : [Py_{13}][FSI] = 1 : 1 : 3	$NaNi_{0.33}Fe_{0.33}Mn_{0.33}O_2$	4.1 V	112
3.04 M $NaPF_6$ in DEGDME/DOL (10 : 1, v/v)	$Na_3V_2(PO_4)_2O_2F$	4.5 V	65
1 M $NaPF_6$ in DEGDME/TEGDME (9 : 1, v/v)	P2-/O3-type layered oxide cathodes	4.3 V	172
1 M $NaPF_6$ in DEGDME	$Na_3(VOPO_4)_2F@rGO$	4.3 V	111
1 M $NaPF_6$ in DEGDME + 0.1 M SPFO (sodium pentadecafluorooctanoate, additive)	$Na_3V_2(PO_4)_3$	4.5 V	173
2 M $NaPF_6$ in DEE	$NaNi_{0.33}Fe_{0.33}Mn_{0.33}O_2$	4.0 V	167
0.6 mM $NaBF_4$ (additive) + 1.2 M $NaPF_6$ in DEGDBE (diethylene glycol dibutyl ether)	$NaNi_{0.3}Fe_{0.4}Mn_{0.3}O_2$	4.1 V	174
0.04 M $NaNO_3$ (Additive) + 1 M NaOTf in DEGDME	$Na_{2/3}Ni_{1/2}Mn_{1/2}O_2$	4.0 V	175
0.5 wt% LiDFBOP + 1 M $NaPF_6$ in FEC/DEC (1 : 9, v/v)	$Na_3V_2(PO_4)_2F_3$	4.5 V	176
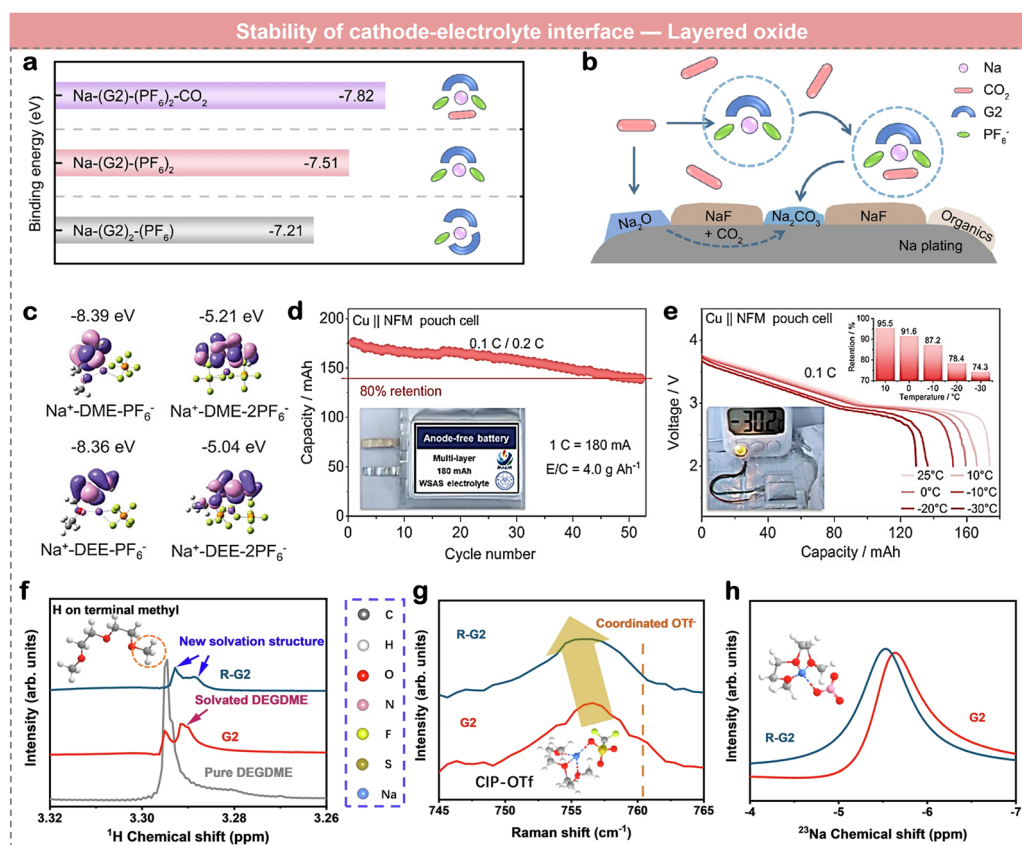
Fig. 11 Analysis of the critical role of ethers in layered oxide cathodes of sodium batteries. (a) and (b) CO_2-regulated solvation structure. Reproduced with permission,[172] Copyright © 2023, American Chemical Society. (c)–(e) Weak solvent structure regulation. Reproduced with permission,[167] Copyright © 2024, Wiley-VCH GmbH. (f)–(h) Additive regulation. Reproduced with permission,[175] Copyright © 2025, The Authors.

dielectric constant and donor/acceptor number are vital to illustrate the solvating power of the solvents in electrolytes, more in-depth experimental data, combined with *in situ* characterization and theoretical calculations, are required to provide a database (ether structure–properties) that quantitatively describes the solvated structure. The additives have broad application prospects in ether-based electrolytes due to their low dosage requirements and excellent effects. Hou *et al.* proposed a rational coupling strategy between perfluorinated-anion additives and cathode/solvent systems, enabling the self-assembly of a protective CEI and

the formation of a robust –C–F···H–C– interaction network to enhance the stability of ether-based electrolytes (Fig. 12(e)–(h)). The preferential adsorption and oxidation of these additives allow the electrolyte to suppress undesirable oxidation at low voltages while maintaining stability at high voltages up to 4.5 V *vs.* Na/Na$^+$. These findings underscore the critical role of sacrificial additives in regulating interfacial stability.[173] To sum up, the optimized ether-based electrolytes enrich systematic options to maintain oxidative stability and compatibility with various cathodes, exhibiting attractive prospects for practical application.
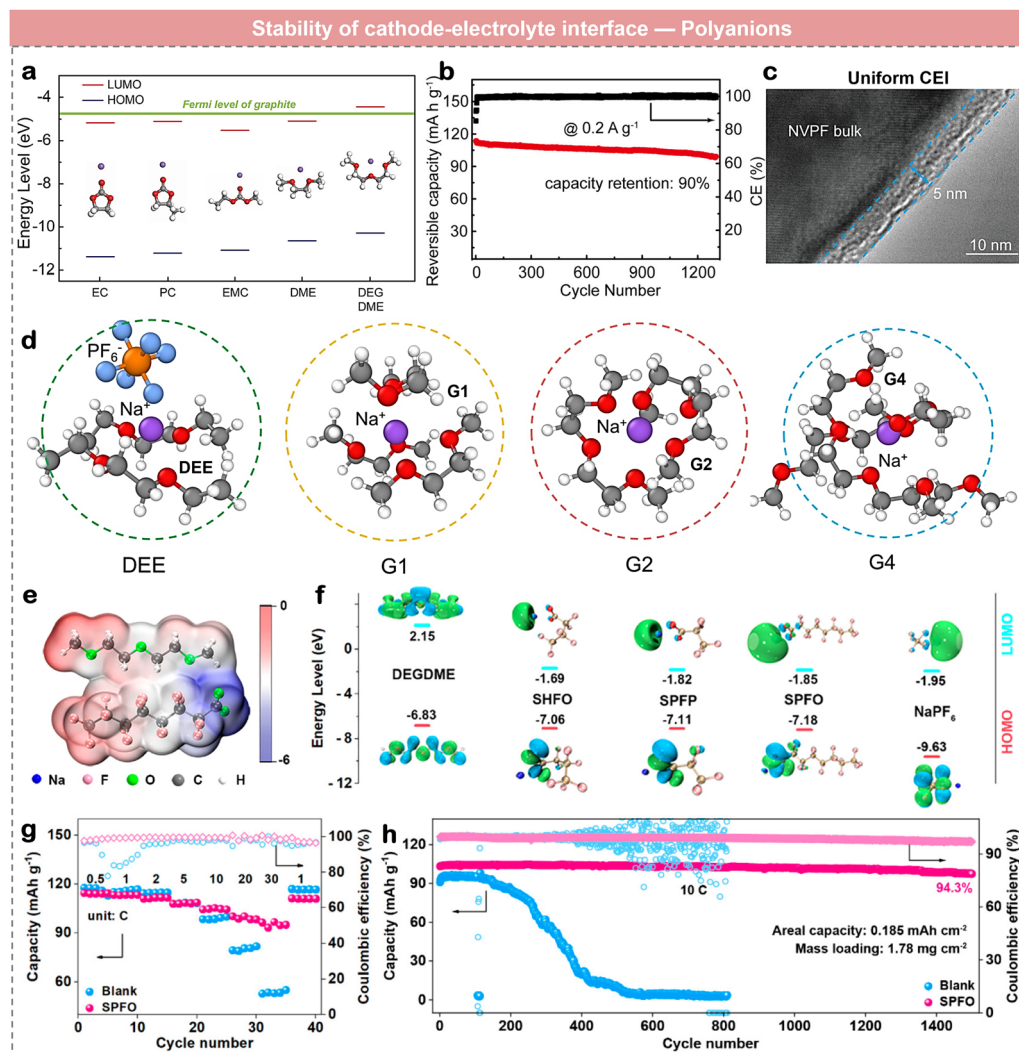
This journal is © The Royal Society of Chemistry 2025

Energy Environ. Sci., 2025, **18**, 6874–6898 | **6889**

Fig. 12 Analysis of the critical role of ethers in polyanion cathodes of sodium batteries. (a)–(c) Salt concentration regulation. Reproduced with permission,[65] © 2021 Wiley-VCH GmbH. (d) Strong solvent structure regulation. Reproduced with permission,[170] Copyright © 2024 Elsevier B.V. (e)–(h) Additive regulation.[173] Reproduced with permission, Copyright © 2024, American Chemical Society.

6. Evolution of commercialization applications

Searching high performance electrolytes for potential commercial applications is a vital prerequisite for realizing high-performance SIBs. In this regard, it is essential to establish imperative guidelines that consider key factors such as electrochemical properties, safety and cost parameters. For ether-based electrolytes, achieving a balance between these attributes, excellent electrochemical performance, high safety, and low cost, is important for their viability in commercial applications (Fig. 13).

6.1 Electrochemical performance

For electrochemical performance, key parameters include ionic conductivity and reductive/oxidative stability of the electrolyte, cycle life, rate performance, and high/low-temperature performance of batteries under practical conditions.

The core competency of ether-based electrolytes lies in their kinetic properties, including excellent rate and low-temperature performance, and high reduction stability compared to commercial ester-based electrolytes. Specifically, ether-based electrolytes (such as DME, DOL, THF, *etc.*) exhibit high ionic conductivity, particularly under low-temperature conditions, which enables superior rate performance. Additionally, these ether-based electrolytes possess a high LUMO energy level, facilitating the formation of a thin and stable SEI, with excellent compatibility with sodium metal. This highlights their unique potential for application in SIBs.[177,178] Nevertheless, the ether-based electrolytes exhibited certain shortcomings in low oxidation stability. They typically undergo decomposition at relatively low voltages (<4.0 V *vs.* Na/Na$^+$), which limits their application in high-voltage cathode materials. Fortunately, the low oxidation stability of ether-based electrolytes can be optimized by adjusting the additive and solvation structure to derive a robust CEI.[179,180] Furthermore, electrochemical performance evaluation in large-capacity full
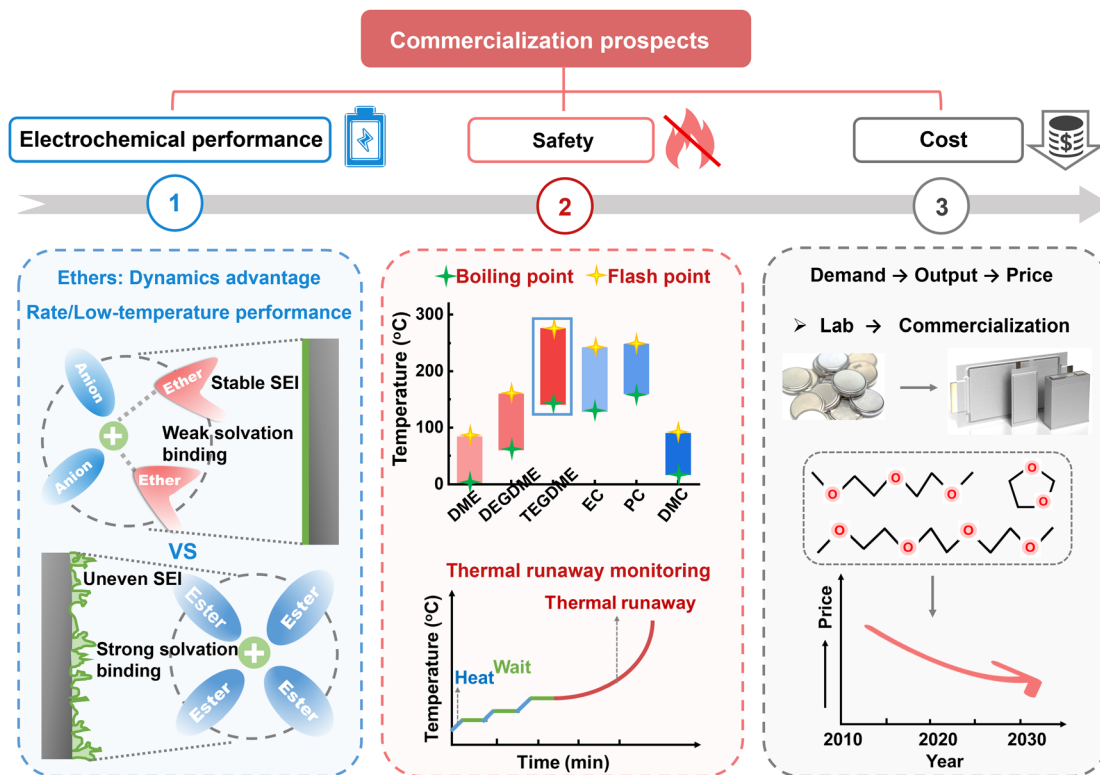
6890 | *Energy Environ. Sci.*, 2025, **18**, 6874–6898

This journal is © The Royal Society of Chemistry 2025

Fig. 13 Evolution of the commercialization prospects of ether-based electrolytes (*vs.* commercial ester-based electrolytes).

batteries should also incorporate performance consistency and manufacturing processes of batteries.

6.2 Safety

Safety concerns in commercial LIBs have been prominent in recent years, with incidents such as battery fires and explosions caused under various abuse conditions. Therefore, improving the safety of batteries has become a critical challenge in this field.

Safety performance can be evaluated in terms of flash point, boiling point, and thermal runaway of ethers.[181] For example, DME solvent, with a lower flash point and boiling point compared to ester-based electrolytes, exhibits poorer thermal stability. This makes them more susceptible to decomposition and vaporization during the early stage of battery self-heating, thus exacerbating the heat accumulation inside batteries.[182,183] Therefore, significant challenges still remain in improving the safety. In contrast, TEGDME has high flash and boiling points similar to commercial ester-based solvents, and has been also shown to be flame-retardant, offering excellent safety performance.[108] Unfortunately, most ether-based and ester-based solvents remain flammable substances, posing certain safety risks. Therefore, it is necessary to incorporate small amounts of flame-retardant additives to mitigate these concerns.

At present, there is still a lack of comparison on thermal runaway properties between ether-based and ester-based electrolytes the under practical conditions. The onset temperature of thermal runaway is closely related to SEI failure,[184] and

improving interfacial stability can mitigate the risk of thermal runaway.[185–187] Therefore, in-depth studies of the mechanisms of thermal runaway and establishing comprehensive battery safety assessment standards are urgently needed.

6.3 Cost

Since the cost is highly related to the demand, ester-based electrolytes benefit from mature production processes, well-established supply chains, and relatively low costs. The price of ethers is currently higher than that of esters due to lower demand and limited production.[188,189] Due to their relatively simple synthesis routes, non-fluorinated ether-based solvents have the potential to achieve cost reductions through scaled-up production in the future.

The highly fluorinated diluents, although important for the study of the low-temperature performance and failure mechanism in SIBs, greatly increase the cost of the electrolyte.[190] In addition to the cost of the electrolyte, the suitability of the ether-based electrolyte preparation process in large-scale production is also crucial for commercialization. For example, researchers have used solvent engineering to design various ether solvents with specific molecular structures, and these ethers have exhibited promising electrochemical performances.[191,192] However, the complex preparation process of the solvents has hindered large-scale preparation, making these solvents unsuitable for commercial use at present. Non-fluorinated linear ethers and cyclic ethers, such as TEGDME and DOL, offer excellent performance at moderate costs.[193] As demand

This journal is © The Royal Society of Chemistry 2025

Energy Environ. Sci., 2025, **18**, 6874–6898 | **6891**

increases and production scales up, the cost is expected to reduce further, facilitating commercialization.

Therefore, while substantial progress has been made, there is still considerable work to be done to meet the commercialization demands for ether-based electrolytes in SIBs. Addressing electrochemical performance, safety and cost, will be key to facilitating the widespread adoption of these ether-based electrolytes.

7. Conclusion and perspectives

SIBs have emerged as one of the most important devices for energy storage, with electrolytes playing a crucial role in their performance. In this review, we first provide an overview of the essential properties of ether as an electrolyte solvent, followed by a comprehensive review of the development history of ether-based electrolytes from their rise, to decline, and eventual revival. This review demonstrates that ether-based electrolytes possess strong core competitiveness in SIBs, particularly due to their advantageous kinetic properties. We then analyzed the characteristics of different ether configurations, including linear ethers, cyclic ethers and fluorinated ethers, and outlined how these variations of ethers influence Na$^+$–solvent, solvent–solvent, and solvent–anion solvation interactions, as well as their impact on battery performance. Among them, linear ethers tend to form strong Na$^+$–solvation structures, while cyclic ethers form moderately strong solvation structures. Fluorinated ethers, on the other hand, promote solvent–solvent and solvent–anion interactions, accelerating Na$^+$ desolvation. This review also discusses the vital effects of ether-based electrolytes in specific anodes and cathodes. For anodes, kinetic advantages in ether-based electrolytes are embodied by a homogeneous SEI, moderate solvation interaction, and ether–Na$^+$ reversible co-embedding. For cathodes, particularly

layered oxides and polyanions, the ether-based electrolyte contributes to high-voltage tolerance by enhancing the interfacial oxidative stability through the formation of an electrolyte-derived CEI. Furthermore, we explore the commercialization prospects of ether-based electrolytes in terms of balanced electrochemical performance, safety and cost. The outlook for commercialization is promising, though challenges remain in addressing safety concerns and the high cost of certain ether-based solvents. Finally, we outline future development directions for ether-based electrolytes in SIBs. These include optimizing solvation structures, enhancing safety mechanisms, and scaling up production processes for cost-effective high-performance electrolytes. Further fundamental and applied research is needed to address these challenges and realize the full potential of ether-based electrolytes in SIBs (Fig. 14). The prospects provided here would serve as a roadmap for advancing the development of next-generation SIBs.

7.1 Performance validation

Ether-based electrolytes must undergo comprehensive evaluation for long cycle life, safety, and high/low-temperature adaptability in large capacity full batteries before commercialization. One of the primary concerns with ether-based electrolytes is their high-voltage stability which directly affects the long-term cycling stability of SIBs, a critical factor for commercial applications. Although constructing a robust CEI can enhance stability, the effectiveness of this improvement in large-capacity batteries remains unverified. Beyond conventional approaches such as additive and solvation structure modulation, recent research shows the importance of inner Helmholtz plane modulation, which plays an important role in optimizing the CEI. Clarifying the coupling effect among solvation structures, additives, and the Helmholtz plane is crucial for designing
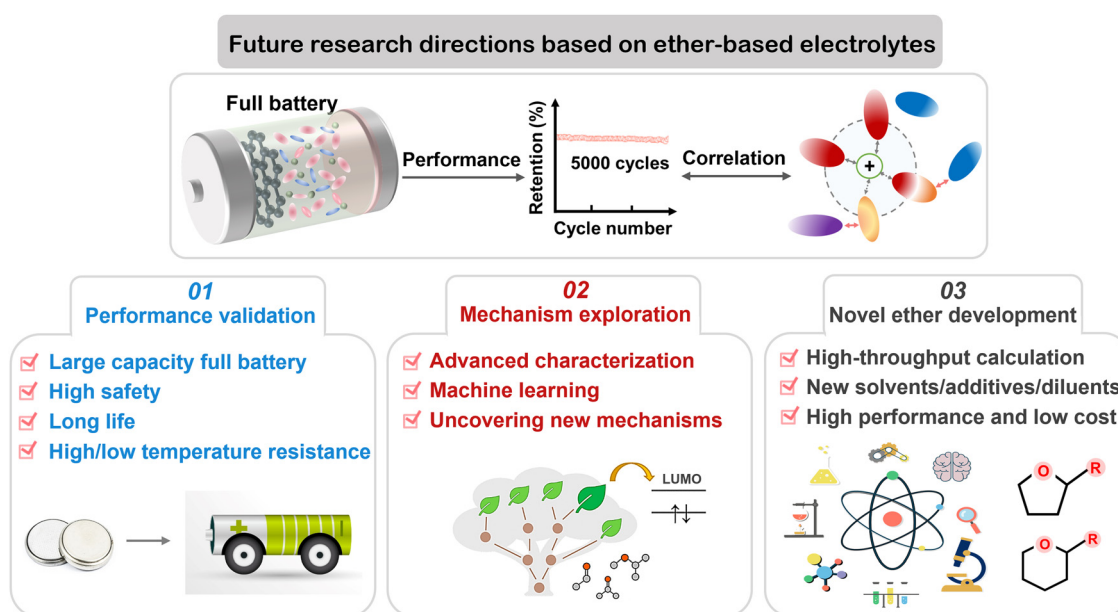

Fig. 14 Future directions of ether-based electrolytes for fundamental and applied research.

6892 | *Energy Environ. Sci.*, 2025, **18**, 6874–6898

This journal is © The Royal Society of Chemistry 2025

a high-quality CEI. Safety performance validation is another critical aspect, especially considering solvents such as DME/DEGDME and other ether solvents, which have a low flash boiling point, present volatility risks and safety hazards. Therefore, these solvents cannot be used alone due to their safety concerns. On the other hand, TEGDME, known for its excellent safety performance, still requires further battery safety testing, such as pinprick, thermal runaway risk assessment. High and low-temperature performance validation is also vital, as energy storage applications put stringent requirements on temperature stability. Ether-based electrolytes, particularly those involving cyclic ethers, may face challenges at high-temperature because of their low boiling point and flash point. In addition, potential ring-opening polymerization reactions of cyclic ether may occur at high temperatures, which reduces the stability of batteries. Therefore, it is necessary to further verify the high and low-temperature adaptability of ether-based electrolytes in large capacity full batteries. Furthermore, SEI layers generated on various electrode surfaces have different compositions and properties, which influence the cycling performance, safety and high/low-temperature performance of SIBs. Currently, film-forming additives in ether-based electrolytes are considered effective for enhancing the interface compatibility. Meanwhile, the formation process of passivation layers in different electrolyte systems should be revealed *via in situ* characterization and advanced theoretical simulation.

7.2 Mechanism exploration

To accelerate the transition of SIBs from the laboratory to commercialization, it is of utmost prominence to understand their reaction and failure mechanisms. Advanced experimental techniques, characterization methods, and theoretical simulation should be used to reveal underlying mechanisms to refine guidelines for improving electrolyte properties. The seemingly contradictory conclusions mentioned above regarding the effect of solvation structure modulation on the battery's modification are due to the lack of clear indicators and definitions of the strength of solvation structures. In addition, the compositional and structural characteristics of high-quality interphases remain unclear, which makes it difficult for researchers to optimize electrolytes and interfaces. The combination of *in situ* characterizations and machine learning to efficiently and accurately analyze the complex interactions behind the battery can help efficiently explore complex interactions within the batteries. Specifically, *in situ* imaging techniques such as optical microscopy (OM), X-ray tomography (XRT) and atomic force microscopy (AFM) are well-developed in batteries, however, *in situ* characterization techniques that could offer higher accuracy, smarter, faster, and more controllable observation areas have great potential to address the challenges in revealing interactions of the electrolytes, such as *in situ* cryo-electron microscopy. Machine learning, which can learn complex relationships between data and build predictive models, is a promising approach to predict the properties of electrolyte solvent molecules, providing an effective and low-cost method to uncover new failure mechanisms and modification mechanisms. Ultimately, there is an urgent need to strengthen fundamental scientific research to reveal the intrinsic action mechanism and optimization methods of ether electrolytes in SIBs to optimize their performance.

7.3 Novel ether development

Technological innovations in electrolyte design are essential for achieving high-performance SIBs. High-throughput calculation based on molecular structure enumeration can assist screening of electrolyte formulation. These simulations can help selecting suitable solvents for different salts by predicting key properties including melting and boiling points, viscosity, dielectric constants, redox properties of novel solvents, salts, additives, and other compounds, therefore helping to efficiently screen electrolyte formulations and identify the most promising configurations for different SIBs. In-depth understanding of the decomposition mechanism of ether solvents under high-voltage conditions would benefit the development of more stable electrolyte systems. Recent research has shown that cyclic ethers with low melting points and weak solvation capabilities exhibit outstanding low-temperature properties. The solvation ability, ion transport, desolvation rate and electrochemical stability of the ether molecules can be regulated by selective methylation, which makes specific functional group substitutions on cyclic ethers a promising route for developing next generation high-performance solvents. Additively, non-fluorinated substitute diluents can effectively reduce the cost while improving kinetic performance. Electrolyte additives, through use in small quantities, can provide significant advantages in enhancing both electrochemical performance and safety. Therefore, the development of next-generation multifunctional novel additives is crucial for advancing SIBs.

In summary, SIBs are effective alternatives to LIBs in large-scale energy storage fields due to their similar properties and lower cost. The electrolyte is one of key components in effectively improving electrochemical performance, but achieving the ultimate performance potential of SIBs requires more than electrolyte optimization alone. The synergetic development of electrolytes and electrodes holds great importance for the successful commercialization of SIBs. In the future, fundamental and applied research on ether-based electrolytes for SIBs must progress simultaneously, and establishing standardized guidelines for evaluating the electrochemical performance and safety performance of ether-based SIBs is indispensable. The development of SIB electrolytes will be a driving force for the commercialization of SIBs.

Author contributions

Data availability

No primary research results, software or code have been included and no new data were generated or analysed as part of this review.

Conflicts of interest

The authors declare no conflicts of interest.

Acknowledgements

References

1 B. Dunn, H. Kamath and J.-M. Tarascon, *Science*, 2011, **334**, 928–934.

2 H. Pan, Y.-S. Hu and L. Chen, *Energy Environ. Sci.*, 2013, **6**, 2338.

3 K. Kubota, M. Dahbi, T. Hosaka, S. Kumakura and S. Komaba, *Chem. Rec.*, 2018, **18**, 459–479.

4 Y. Li, Y. Lu, P. Adelhelm, M.-M. Titirici and Y.-S. Hu, *Chem. Soc. Rev.*, 2019, **48**, 4655–4687.

5 L. Wang, J. Zhu, N. Li, Z. Zhang, S. Zhang, Y. Chen, J. Zhang, Y. Yang, L. Tan, X. Niu, X. Wang, X. Ji and Y. Zhu, *Energy Environ. Sci.*, 2024, **17**, 3470–3481.

6 K. Mizushima, P. C. Jones, P. J. Wiseman and J. B. Goodenough, *Mater. Res. Bull.*, 1980, **16**, 783–789.

7 Y. A, S. K and N. T, 198929 3[P], 1985.

8 R. Yazami and P. Touzain, *J. Power Sources*, 1983, **9**, 365–371.

9 R. Fong, U. y Sacken and J. R. Dahn, *J. Electrochem. Soc.*, 1990, **137**, 2009–2013.

10 C. A. Vincent, *Philos. Trans. R. Soc., A*, 1996, **354**, 1567–1576.

11 E. Paled, *J. Electrochem. Soc.*, 1979, **126**, 2047–2051.

12 E. Peled, *J. Power Sources*, 1983, **9**, 253–266.

13 Y. Yamada and A. Yamada, *J. Electrochem. Soc.*, 2015, **162**, A2406–A2423.

14 R. Cui, Y. Ma, X. Gao, W. Wang, J. Wang, Z. Xing and Z. Ju, *Energy Storage Mater.*, 2024, **71**, 103627.

15 B. Jache and P. Adelhelm, *Angew. Chem., Int. Ed.*, 2014, **53**, 10169–10173.

16 M. Qin, Z. Zeng, Q. Wu, H. Yan, M. Liu, Y. Wu, H. Zhang, S. Lei, S. Cheng and J. Xie, *Energy Environ. Sci.*, 2023, **16**, 546–556.

17 Q. Li, G. Liu, H. Cheng, Q. Sun, J. Zhang and J. Ming, *Chem. – Eur. J.*, 2021, **27**, 15842–15865.

18 N. Piao, X. Gao, H. Yang, Z. Guo, G. Hu, H.-M. Cheng and F. Li, *eTransportation*, 2022, **11**, 100145.

19 X. Chen, J. Tian, P. Li, Y. Fang, Y. Fang, X. Liang, J. Feng, J. Dong, X. Ai, H. Yang and Y. Cao, *Adv. Energy Mater.*, 2022, **12**, 2200886.

20 Y. Chu, J. Zhang, Y. Zhang, Q. Li, Y. Jia, X. Dong, J. Xiao, Y. Tao and Q. H. Yang, *Adv. Mater.*, 2023, **35**, 2212186.

21 L. Tao, D. Xia, P. Sittisomwong, H. Zhang, J. Lai, S. Hwang, T. Li, B. Ma, A. Hu, J. Min, D. Hou, S. R. Shah, K. Zhao, G. Yang, H. Zhou, L. Li, P. Bai, F. Shi and F. Lin, *J. Am. Chem. Soc.*, 2024, **146**, 16764–16774.

22 Y.-C. Gao, N. Yao, X. Chen, L. Yu, R. Zhang and Q. Zhang, *J. Am. Chem. Soc.*, 2023, **145**, 23764–23770.

23 T. Sun, X. L. Feng, Q. Q. Sun, Y. Yu, G. B. Yuan, Q. Xiong, D. P. Liu, X. B. Zhang and Y. Zhang, *Angew. Chem., Int. Ed.*, 2021, **60**, 26806–26812.

24 G. Yoon, H. Kim, I. Park and K. Kang, *Adv. Energy Mater.*, 2016, **7**, 1601519.

25 Y. S. Meng, V. Srinivasan and K. Xu, *Science*, 2022, **378**, 1065.

26 E. Peled, D. Golodnitsky and G. Ardel, *J. Electrochem. Soc.*, 1997, **144**, 208–210.

27 E. Peled, D. Golodnitsky, G. Ardel and V. Eshkenazy, *Electrochim. Acta*, 1995, **40**, 2197–2204.

28 A. Zaban, E. Zinigrad and D. Aurbach, *J. Phys. Chem.*, 1996, **100**, 3089–3101.

29 M. Li, C. Wang, Z. Chen, K. Xu and J. Lu, *Chem. Rev.*, 2020, **120**, 6783–6819.

30 M. Winter, B. Barnett and K. Xu, *Chem. Rev.*, 2018, **118**, 11433–11456.

31 K. Xu, *Chem. Rev.*, 2004, **104**, 4303–4417.

32 K. Edström, T. Gustafsson and J. O. Thomas, *Electrochim. Acta*, 2004, **50**, 397–403.

33 L. L. Jiang, C. Yan, Y. X. Yao, W. Cai, J. Q. Huang and Q. Zhang, *Angew. Chem., Int. Ed.*, 2021, **60**, 3402–3406.

34 X. q Zhang, X. Chen, L. p Hou, B. q Li, X. b Cheng, J. q Huang and Q. Zhang, *ACS Energy Lett.*, 2019, **4**, 411–416.

35 J. B. Goodenough, *Nat. Electron.*, 2018, **1**, 204.

36 J. M. Tarascon and M. Armand, *Nature*, 2001, **414**, 359–368.

37 H. Cheng, Q. Sun, L. Li, Y. Zou, Y. Wang, T. Cai, F. Zhao, G. Liu, Z. Ma, W. Wahyudi, Q. Li and J. Ming, *ACS Energy Lett.*, 2022, **7**, 490–513.

38 S. Zhang, G. Yang, Z. Liu, X. Li, X. Wang, R. Chen, F. Wu, Z. Wang and L. Chen, *Nano Lett.*, 2021, **21**, 3310–3317.

39 J. Hu, Y. Ji, G. Zheng, W. Huang, Y. Lin, L. Yang and F. Pan, *Aggregate*, 2022, **3**, e153.

40 H. Chen, K. Chen, J. Yang, B. Liu, L. Luo, H. Li, L. Chen, A. Zhao, X. Liang, J. Feng, Y. Fang and Y. Cao, *J. Am. Chem. Soc.*, 2024, **146**, 15751–15760.

41 K. Xu, *J. Power Sources*, 2023, **559**, 232652.

42 B. Li, Y. Chao, M. Li, Y. Xiao, R. Li, K. Yang, X. Cui, G. Xu, L. Li, C. Yang, Y. Yu, D. P. Wilkinson and J. Zhang, *Electrochem. Energy Rev.*, 2023, **6**, 7.

43 X. Pu, S. Zhang, D. Zhao, Z.-L. Xu, Z. Chen and Y. Cao, *Electrochem. Energy Rev.*, 2024, **7**, 21.

44 W. Tang, R. Qi, J. Wu, Y. Zuo, Y. Shi, R. Liu, W. Yan and J. Zhang, *Electrochem. Energy Rev.*, 2024, **7**, 23.

45 Y. Li, Y. Li, A. Pei, K. Yan, Y. Sun, C.-L. Wu, L.-M. Joubert, R. Chin, A. L. Koh, Y. Yu, J. Perrino, B. Butz, S. Chu and Y. Cui, *Science*, 2017, **358**, 506–510.

46 Z. Zhang, Y. Li, R. Xu, W. Zhou, Y. Li, S. T. Oyakhire, Y. Wu, J. Xu, H. Wang, Z. Yu, D. T. Boyle, W. Huang, Y. Ye, H. Chen, J. Wan, Z. Bao, W. Chiu and Y. Cui, *Science*, 2022, **375**, 66–70.

6894 | *Energy Environ. Sci.*, 2025, **18**, 6874–6898

This journal is © The Royal Society of Chemistry 2025

47 S. Tan, Z. Shadike, X. Cai, R. Lin, A. Kludze, O. Borodin, B. L. Lucht, C. Wang, E. Hu, K. Xu and X.-Q. Yang, *Electrochem. Energy Rev.*, 2023, **6**, 35.

48 S. Tan, Z. Shadike, X. Cai, R. Lin, A. Kludze, O. Borodin, B. L. Lucht, C. Wang, E. Hu, K. Xu and X.-Q. Yang, *Electrochem. Energy Rev.*, 2024, **7**, 4.

49 L. G. Zhuo, W. Liao and Z. X. Yu, *Asian J. Org. Chem.*, 2012, **1**, 336–345.

50 E. Wang, Y. Niu, Y.-X. Yin and Y.-G. Guo, *ACS Mater. Lett.*, 2020, **3**, 18–41.

51 P. Liang, J. Li, Y. Dong, Z. Wang, G. Ding, K. Liu, L. Xue and F. Cheng, *Angew. Chem., Int. Ed.*, 2024, e202415853.

52 K. Cui, R. Hou, H. Zhou and S. Guo, *Adv. Funct. Mater.*, 2024, 2419275.

53 M. S. Whittingham, *Science*, 1976, **192**, 1126–1127.

54 J. R. Owen, *Chem. Soc. Rev.*, 1997, **26**, 259–267.

55 D. A. Stevens and J. R. Dahn, *J. Electrochem. Soc.*, 2000, **147**, 1271–1273.

56 H. Kim, J. Hong, Y. U. Park, J. Kim, I. Hwang and K. Kang, *Adv. Funct. Mater.*, 2014, **25**, 534–541.

57 B. H. Hou, Y. Y. Wang, Q. L. Ning, W. H. Li, X. T. Xi, X. Yang, H. J. Liang, X. Feng and X. L. Wu, *Adv. Mater.*, 2019, **31**, 1903125.

58 K. Li, J. Zhang, D. Lin, D.-W. Wang, B. Li, W. Lv, S. Sun, Y.-B. He, F. Kang, Q.-H. Yang, L. Zhou and T.-Y. Zhang, *Nat. Commun.*, 2019, **10**, 725.

59 Z. W. Seh, J. Sun, Y. Sun and Y. Cui, *ACS Cent. Sci.*, 2015, **1**, 449–455.

60 Y. X. Wang, B. Zhang, W. Lai, Y. Xu, S. L. Chou, H. K. Liu and S. X. Dou, *Adv. Energy Mater.*, 2017, **7**, 1602829.

61 J. Zhang, D.-W. Wang, W. Lv, S. Zhang, Q. Liang, D. Zheng, F. Kang and Q.-H. Yang, *Energy Environ. Sci.*, 2017, **10**, 370–376.

62 J. Zheng, S. Chen, W. Zhao, J. Song, M. H. Engelhard and J.-G. Zhang, *ACS Energy Lett.*, 2018, **3**, 315–321.

63 Z. Zhu, F. Cheng, Z. Hu, Z. Niu and J. Chen, *J. Power Sources*, 2015, **293**, 626–634.

64 R. Dong, L. Zheng, Y. Bai, Q. Ni, Y. Li, F. Wu, H. Ren and C. Wu, *Adv. Mater.*, 2021, **33**, 2008810.

65 H. J. Liang, Z. Y. Gu, X. X. Zhao, J. Z. Guo, J. L. Yang, W. H. Li, B. Li, Z. M. Liu, W. L. Li and X. L. Wu, *Angew. Chem., Int. Ed.*, 2021, **60**, 26837–26846.

66 C. Wang, A. C. Thenuwara, J. Luo, P. P. Shetty, M. T. McDowell, H. Zhu, S. Posada-Perez, H. Xiong, G. Hautier and W. Li, *Nat. Commun.*, 2022, **13**, 4934.

67 Q. Yao, C. Zheng, D. Ji, Y. Du, J. Su, N. Wang, J. Yang, S. Dou and Y. Qian, *Proc. Natl. Acad. Sci. U. S. A.*, 2024, **121**, e2312337121.

68 C. Yang, X. Liu, Y. Lin, L. Yin, J. Lu and Y. You, *Adv. Mater.*, 2023, **35**, e2301817.

69 M. Wang, L. Yin, M. Zheng, X. Liu, C. Yang, W. Hu, J. Xie, R. Sun, J. Han, Y. You and J. Lu, *Nat. Commun.*, 2024, **15**, 8866.

70 M. Fei, L. Qi, S. Han, Y. Li, H. Xi, Z. Lin, J. Wang, C. Ducati, M. Chhowalla, R. V. Kumar, Y. Jin and J. Zhu, *Angew. Chem., Int. Ed.*, 2024, **63**, e202409719.

71 H. Liang, P. Kumar, Z. Ma, F. Zhao, H. Cheng, H. Xie, Z. Cao, L. Cavallo, Q. Li and J. Ming, *ACS Energy Lett.*, 2024, **9**, 3536–3546.

72 B. Nan, L. Chen, N. D. Rodrigo, O. Borodin, N. Piao, J. Xia, T. Pollard, S. Hou, J. Zhang, X. Ji, J. Xu, X. Zhang, L. Ma, X. He, S. Liu, H. Wan, E. Hu, W. Zhang, K. Xu, X. Q. Yang, B. Lucht and C. Wang, *Angew. Chem., Int. Ed.*, 2022, **61**, e202205967.

73 Q. Sun, Z. Cao, Z. Ma, J. Zhang, H. Cheng, X. Guo, G.-T. Park, Q. Li, E. Xie, L. Cavallo, Y.-K. Sun and J. Ming, *ACS Energy Lett.*, 2022, **7**, 3545–3556.

74 Z. Yang, J. He, W. H. Lai, J. Peng, X. H. Liu, X. X. He, X. F. Guo, L. Li, Y. Qiao, J. M. Ma, M. Wu and S. L. Chou, *Angew. Chem., Int. Ed.*, 2021, **60**, 27086–27094.

75 X. Zhou, Q. Zhang, Z. Zhu, Y. Cai, H. Li and F. Li, *Angew. Chem., Int. Ed.*, 2022, **61**, e202205045.

76 Z. Tang, S. Zhou, Y. Huang, H. Wang, R. Zhang, Q. Wang, D. Sun, Y. Tang and H. Wang, *Electrochem. Energy Rev.*, 2023, **6**, 8.

77 Y. Wu, W. Shuang, Y. Wang, F. Chen, S. Tang, X.-L. Wu, Z. Bai, L. Yang and J. Zhang, *Electrochem. Energy Rev.*, 2024, **7**, 17.

78 H. Adenusi, G. A. Chass, S. Passerini, K. V. Tian and G. Chen, *Adv. Energy Mater.*, 2023, **13**, 2203307.

79 A. Ponrouch, E. Marchante, M. Courty, J.-M. Tarascon and M. R. Palacín, *Energy Environ. Sci.*, 2012, **5**, 8572–8583.

80 X. Zhou, Y. Zhou, L. Yu, L. Qi, K.-S. Oh, P. Hu, S.-Y. Lee and C. Chen, *Chem. Soc. Rev.*, 2024, **53**, 5291–5337.

81 G. G. Eshetu, G. A. Elia, M. Armand, M. Forsyth, S. Komaba, T. Rojo and S. Passerini, *Adv. Energy Mater.*, 2020, **10**, 2000093.

82 Y. Li, F. Wu, Y. Li, M. Liu, X. Feng, Y. Bai and C. Wu, *Chem. Soc. Rev.*, 2022, **51**, 4484–4536.

83 H. Fujimoto and S. Satoh, *J. Phys. Chem.*, 1994, **98**, 1436–1441.

84 J.-G. Han, J. B. Lee, A. Cha, T. K. Lee, W. Cho, S. Chae, S. J. Kang, S. K. Kwak, J. Cho, S. Y. Hong and N.-S. Choi, *Energy Environ. Sci.*, 2018, **11**, 1552–1562.

85 Y. Wang, P. Bai, B. Li, C. Zhao, Z. Chen, M. Li, H. Su, J. Yang and Y. Xu, *Adv. Energy Mater.*, 2021, **11**, 2101972.

86 G. Xu, C. Pang, B. Chen, J. Ma, X. Wang, J. Chai, Q. Wang, W. An, X. Zhou, G. Cui and L. Chen, *Adv. Energy Mater.*, 2017, **8**, 1701398.

87 B. Qiu, J. Wang, Y. Xia, Z. Wei, S. Han and Z. Liu, *ACS Appl. Mater. Interfaces*, 2014, **6**, 9185–9193.

88 V. Gutmann, *Electrochim. Acta*, 1976, **21**, 661–670.

89 U. Mayer, V. Gutmann and W. Gerger, *Monatsh. Chem.*, 1975, **106**, 1235–1257.

90 Y. L. K. Xu, S. S. Zhang, T. Richard Jow and T. B. Curtis, *J. Phys. Chem. C*, 2007, **111**, 7411–7421.

91 C. Chen, M. Wu, J. Liu, Z. Xu, K. Zaghib and Y. Wang, *J. Power Sources*, 2020, **471**, 228455.

92 J. Xu, J. Zhang, T. P. Pollard, Q. Li, S. Tan, S. Hou, H. Wan, F. Chen, H. He, E. Hu, K. Xu, X. Q. Yang, O. Borodin and C. Wang, *Nature*, 2023, **614**, 694–700.

93 B. Sayahpour, W. Li, S. Bai, B. Lu, B. Han, Y.-T. Chen, G. Deysher, S. Parab, P. Ridley, G. Raghavendran, L. H. B. Nguyen, M. Zhang and Y. S. Meng, *Energy Environ. Sci.*, 2024, **17**, 1216–1228.

94 J. Tan, J. Matz, P. Dong, J. Shen and M. Ye, *Adv. Energy Mater.*, 2021, **11**, 2100046.

95 Y. Chen, C. Ye, N. Zhang, J. Liu, H. Li, K. Davey and S.-Z. Qiao, *Mater. Today*, 2024, **73**, 260–274.

96 K. Chen, X. Shen, L. Luo, H. Chen, R. Cao, X. Feng, W. Chen, Y. Fang and Y. Cao, *Angew. Chem., Int. Ed.*, 2023, **62**, e202312373.

97 J. G. Han, K. Kim, Y. Lee and N. S. Choi, *Adv. Mater.*, 2019, **31**, e1804822.

98 H. J. Liang, Z. Y. Gu, X. X. Zhao, J. Z. Guo, J. L. Yang, W. H. Li, B. Li, Z. M. Liu, W. L. Li and X. L. Wu, *Angew. Chem., Int. Ed.*, 2021, **60**, 26837–26846.

99 R. Dong, L. Zheng, Y. Bai, Q. Ni, Y. Li, F. Wu, H. Ren and C. Wu, *Adv. Mater.*, 2021, **33**, e2008810.

100 T. Abe, H. Fukuda, Y. Iriyama and Z. Ogumi, *J. Electrochem. Soc.*, 2004, **151**, A1120–A1123.

101 P. Xiao, X. Yun, Y. Chen, X. Guo, P. Gao, G. Zhou and C. Zheng, *Chem. Soc. Rev.*, 2023, **52**, 5255–5316.

102 J. Xu, V. Koverga, A. Phan, A. Min Li, N. Zhang, M. Baek, C. Jayawardana, B. L. Lucht, A. T. Ngo and C. Wang, *Adv. Mater.*, 2023, **36**, 2306462.

103 Y. Huang, L. Zhao, L. Li, M. Xie, F. Wu and R. Chen, *Adv. Mater.*, 2019, **31**, 1808393.

104 J. Xiang and Y.-C. Lu, *ACS Nano*, 2024, **18**, 10726–10737.

105 N. von Aspern, G. V. Röschenthaler, M. Winter and I. Cekic-Laskovic, *Angew. Chem., Int. Ed.*, 2019, **58**, 15978–16000.

106 H. Wan, J. Xu and C. Wang, *Nat. Rev. Chem.*, 2023, **8**, 30–44.

107 Y. Wang, X. Yang, Y. Meng, Z. Wen, R. Han, X. Hu, B. Sun, F. Kang, B. Li, D. Zhou, C. Wang and G. Wang, *Chem. Rev.*, 2024, **124**, 3494–3589.

108 D. Di Lecce, L. Carbone, V. Gancitano and J. Hassoun, *J. Power Sources*, 2016, **334**, 146–153.

109 N. Zhang, T. Deng, S. Zhang, C. Wang, L. Chen, C. Wang and X. Fan, *Adv. Mater.*, 2022, **34**, 2107899.

110 Y. Li, Q. Zhou, S. Weng, F. Ding, X. Qi, J. Lu, Y. Li, X. Zhang, X. Rong, Y. Lu, X. Wang, R. Xiao, H. Li, X. Huang, L. Chen and Y.-S. Hu, *Nat. Energy*, 2022, **7**, 511–519.

111 D. Ba, Q. Gui, W. Liu, Z. Wang, Y. Li and J. Liu, *Nano Energy*, 2022, **94**, 106918.

112 Y. Liu, S. Lu, Z. Wang, J. Xu, S. Weng, J. Xue, H. Tu, F. Zhang, L. Liu, Y. Gao, H. Li, J. Zheng and X. Wu, *Adv. Funct. Mater.*, 2024, **34**, 2312295.

113 X. Yi, X. Li, J. Zhong, S. Wang, Z. Wang, H. Guo, J. Wang and G. Yan, *Adv. Funct. Mater.*, 2022, **32**, 2209523.

114 Y. H. Feng, M. Liu, J. Wu, C. Yang, Q. Liu, Y. Tang, X. Zhu, G. X. Wei, H. Dong, X. Y. Fan, S. F. Chen, W. Hao, L. Yu, X. Ji, Y. You, P. F. Wang and J. Lu, *Angew. Chem., Int. Ed.*, 2024, **63**, e202403585.

115 J. Li, J. Hao, Q. Yuan, R. Wang, F. Marlton, T. Wang, C. Wang, X. Guo and G. Wang, *Carbon Energy*, 2024, **6**, e518.

116 J. Wang, J. Hu, F. Kang and D. Zhai, *Energy Environ. Sci.*, 2024, **17**, 3202–3209.

117 M. Ma, H. Cai, C. Xu, R. Huang, S. Wang, H. Pan and Y. S. Hu, *Adv. Funct. Mater.*, 2021, **31**, 2100278.

118 S. Wang, S. Weng, X. Li, Y. Liu, X. Huang, Y. Jie, Y. Pan, H. Zhou, S. Jiao, Q. Li, X. Wang, T. Cheng, R. Cao and D. Xu, *Angew. Chem., Int. Ed.*, 2023, **62**, e202313447.

119 Q. Zhu, D. Yu, J. Chen, L. Cheng, M. Tang, Y. Wang, Y. Li, J. Yang and H. Wang, *Joule*, 2024, **8**, 482–495.

120 X. Yi, X. Li, J. Zhong, Z. Cui, Z. Wang, H. Guo, J. Wang and G. Yan, *ACS Appl. Mater. Interfaces*, 2024, **16**, 11585–11594.

121 X. Hu, E. Matios, Y. Zhang, C. Wang, J. Luo and W. Li, *Angew. Chem., Int. Ed.*, 2021, **60**, 5978–5983.

122 H. Fang, Y. Huang, W. Hu, Z. Song, X. Wei, J. Geng, Z. Jiang, H. Qu, J. Chen and F. Li, *Angew. Chem., Int. Ed.*, 2024, **63**, e202400539.

123 L. Hu, J. Deng, Y. Lin, Q. Liang, B. Ge, Q. Weng, Y. Bai, Y. Li, Y. Deng, G. Chen and X. Yu, *Adv. Mater.*, 2024, **36**, 2312161.

124 X. Zhou, X. Chen, W. Kuang, W. Zhu, X. Zhang, X. Liu, X. Wu, L. Zhang, C. Zhang, L. Li, J. Wang and S. L. Chou, *Angew. Chem., Int. Ed.*, 2024, **63**, e202410494.

125 R. R. Vaidyula, M. H. Nguyen, J. A. Weeks, Y. Wang, Z. Wang, K. Kawashima, A. G. Paul-Orecchio, H. Celio, A. Dolocan, G. Henkelman and C. B. Mullins, *Adv. Mater.*, 2024, **36**, 2312508.

126 J. Li, S. Sui, X. Zhou, K. Lei, Q. Yang, S. Chu, L. Li, Y. Zhao, M. Gu, S. Chou and S. Zheng, *Angew. Chem., Int. Ed.*, 2024, **63**, e202400406.

127 Y. Jin, Y. Xu, P. M. L. Le, T. D. Vo, Q. Zhou, X. Qi, M. H. Engelhard, B. E. Matthews, H. Jia, Z. Nie, C. Niu, C. Wang, Y. Hu, H. Pan and J.-G. Zhang, *ACS Energy Lett.*, 2020, **5**, 3212–3220.

128 Y. H. Feng, M. Liu, W. Qi, H. Liu, Q. Liu, C. Yang, Y. Tang, X. Zhu, S. Sun, Y. M. Li, T. L. Chen, B. Xiao, X. Ji, Y. You and P. F. Wang, *Angew. Chem., Int. Ed.*, 2024, **63**, e202415644.

129 G. G. Eshetu, S. Grugeon, H. Kim, S. Jeong, L. Wu, G. Gachot, S. Laruelle, M. Armand and S. Passerini, *ChemSusChem*, 2016, **9**, 462–471.

130 A. Bhide, J. Hofmann, A. K. Durr, J. Janek and P. Adelhelm, *Phys. Chem. Chem. Phys.*, 2014, **16**, 1987–1998.

131 F. Cheng, M. Cao, Q. Li, C. Fang, J. Han and Y. Huang, *ACS Nano*, 2023, **17**, 18608–18615.

132 V. Aravindan, J. Gnanaraj, S. Madhavi and H. K. Liu, *Chem. – Eur. J.*, 2011, **17**, 14326–14346.

133 Y. Li, A. Vasileiadis, Q. Zhou, Y. Lu, Q. Meng, Y. Li, P. Ombrini, J. Zhao, Z. Chen, Y. Niu, X. Qi, F. Xie, R. van der Jagt, S. Ganapathy, M.-M. Titirici, H. Li, L. Chen, M. Wagemaker and Y.-S. Hu, *Nat. Energy*, 2024, **9**, 134–142.

134 Y. Wan, Y. Liu, D. Chao, W. Li and D. Zhao, *Nano Mater. Sci*, 2023, **5**, 189–201.

135 G. Yang, X. Li, Z. Guan, Y. Tong, B. Xu, X. Wang, Z. Wang and L. Chen, *Nano Lett.*, 2020, **20**, 3836–3843.

136 J. B. Goodenough and Y. Kim, *Chem. Mater.*, 2009, **22**, 587–603.

6896 | *Energy Environ. Sci.*, 2025, **18**, 6874–6898

This journal is © The Royal Society of Chemistry 2025

137 A. Zeng, Y. He, M. Qin, C. Hu, F. Huang, J. Qiu, S. Liang, Y. Sun and G. Fang, *Energy Storage Mater.*, 2025, **74**, 103894.

138 Z. Tang, H. Wang, P. F. Wu, S. Y. Zhou, Y. C. Huang, R. Zhang, D. Sun, Y. G. Tang and H. Y. Wang, *Angew. Chem., Int. Ed.*, 2022, **61**, e202200475.

139 B. Ge, J. Deng, Z. Wang, Q. Liang, L. Hu, X. Ren, R. Li, Y. Lin, Y. Li, Q. Wang, B. Han, Y. Deng, X. Fan, B. Li, G. Chen and X. Yu, *Adv. Mater.*, 2024, **36**, 2408161.

140 F. Huang, P. Xu, G. Fang and S. Liang, *Adv. Mater.*, 2024, **36**, 2402284.

141 Z. Li, L. Miao, G. Lin, W. Tian, S. Yuan, Y. Si, Q. Wang and L. Jiao, *Adv. Energy Mater.*, 2024, **14**, 2402284.

142 S. Wan, K. Song, J. Chen, S. Zhao, W. Ma, W. Chen and S. Chen, *J. Am. Chem. Soc.*, 2023, **145**, 21661–21671.

143 H. Wang, J. Wang, W. Li, J. Hu, J. Dong, D. Zhai and F. Kang, *Adv. Mater.*, 2024, **36**, 2409062.

144 R. Zhuang, X. Zhang, C. Qu, X. Xu, J. Yang, Q. Ye, Z. Liu, S. Kaskel, F. Xu and H. Wang, *Sci. Adv.*, 2023, **9**, eadh8060.

145 P. Xu, F. Huang, Y. Sun, Y. Lei, X. Cao, S. Liang and G. Fang, *Adv. Funct. Mater.*, 2024, **34**, 2406080.

146 Y. Sun, J.-C. Li, H. Zhou and S. Guo, *Energy Environ. Sci.*, 2023, **16**, 4759–4811.

147 C. Li, H. Xu, L. Ni, B. Qin, Y. Ma, H. Jiang, G. Xu, J. Zhao and G. Cui, *Adv. Energy Mater.*, 2023, **13**, 2301758.

148 E. Goikolea, V. Palomares, S. Wang, I. R. de Larramendi, X. Guo, G. Wang and T. Rojo, *Adv. Energy Mater.*, 2020, **10**, 2002055.

149 Z. Lu, H. Yang, Y. Guo, H. Lin, P. Shan, S. Wu, P. He, Y. Yang, Q.-H. Yang and H. Zhou, *Nat. Commun.*, 2024, **15**, 3497.

150 X. Yin, Z. Wang, Y. Liu, Z. Lu, H. Long, T. Liu, J. Zhang and Y. Zhao, *Nano Res.*, 2023, **16**, 10922–10930.

151 B. Qin, Y. Ma, C. Li, H. Xu, J. Li, B. Xie, X. Du, S. Dong, G. Xu and G. Cui, *Energy Storage Mater.*, 2023, **61**, 102891.

152 J. Kim, J. Kim, J. Jeong, J. Park, C.-Y. Park, S. Park, S. G. Lim, K. T. Lee, N.-S. Choi, H. R. Byon, C. Jo and J. Lee, *Energy Environ. Sci.*, 2022, **15**, 4109–4118.

153 S. Wang, S. Weng, X. Li, Y. Liu, X. Huang, Y. Jie, Y. Pan, H. Zhou, S. Jiao, Q. Li, X. Wang, T. Cheng, R. Cao and D. Xu, *Angew. Chem., Int. Ed.*, 2023, **135**, e202313447.

154 F. Ding, P. Ji, Z. Han, X. Hou, Y. Yang, Z. Hu, Y. Niu, Y. Liu, J. Zhang, X. Rong, Y. Lu, H. Mao, D. Su, L. Chen and Y.-S. Hu, *Nat. Energy*, 2024, **9**, 1529–1539.

155 Y.-J. Guo, R.-X. Jin, M. Fan, W.-P. Wang, S. Xin, L.-J. Wan and Y.-G. Guo, *Chem. Soc. Rev.*, 2024, **53**, 7828–7874.

156 J. Peng, W. Zhang, Q. Liu, J. Wang, S. Chou, H. Liu and S. Dou, *Adv. Mater.*, 2022, **34**, 2108384.

157 H. Zhang, Y. Gao, X. Liu, L. Zhou, J. Li, Y. Xiao, J. Peng, J. Wang and S. L. Chou, *Adv. Energy Mater.*, 2023, **13**, 2300149.

158 F. Xiong, J. Li, C. Zuo, X. Zhang, S. Tan, Y. Jiang, Q. An, P. K. Chu and L. Mai, *Adv. Funct. Mater.*, 2022, **33**, 2211257.

159 T. Yuan, Y. Wang, J. Zhang, X. Pu, X. Ai, Z. Chen, H. Yang and Y. Cao, *Nano Energy*, 2019, **56**, 160–168.

160 X. Fan and C. Wang, *Chem. Soc. Rev.*, 2021, **50**, 10486–10566.

161 A. Bouibes, N. Takenaka, T. Fujie, K. Kubota, S. Komaba and M. Nagaoka, *ACS Appl. Mater. Interfaces*, 2018, **10**, 28525–28532.

162 V. Simone, L. Lecarme, L. Simonin and S. Martinet, *J. Electrochem. Soc.*, 2016, **164**, A145–A150.

163 X. Liu, J. Zhao, H. Dong, L. Zhang, H. Zhang, Y. Gao, X. Zhou, L. Zhang, L. Li, Y. Liu, S. Chou, W. Lai, C. Zhang and S. Chou, *Adv. Funct. Mater.*, 2024, **34**, 2402310.

164 D. S. Hall, T. Hynes, C. P. Aiken and J. R. Dahn, *J. Electrochem. Soc.*, 2020, **167**, 100538.

165 Z. Li, L. P. Hou, N. Yao, X. Y. Li, Z. X. Chen, X. Chen, X. Q. Zhang, B. Q. Li and Q. Zhang, *Angew. Chem., Int. Ed.*, 2023, **62**, e202309968.

166 Y. F. Tian, S. J. Tan, Z. Y. Lu, D. X. Xu, H. X. Chen, C. H. Zhang, X. S. Zhang, G. Li, Y. M. Zhao, W. P. Chen, Q. Xu, R. Wen, J. Zhang and Y. G. Guo, *Angew. Chem., Int. Ed.*, 2023, **62**, e202305988.

167 Y. Zou, B. Zhang, H. Luo, X. Yu, M. Yang, Q. Zheng, J. Wang, C. Jiao, Y. Chen, H. Zhang, J. Xue, X. Kuai, H. G. Liao, C. Ouyang, Z. Ning, Y. Qiao and S. G. Sun, *Adv. Mater.*, 2024, **36**, 2410261.

168 S. Chen, Z. Deng, J. Li, W. Zhao, B. Nan, Y. Zuo, J. Fang, Y. Huang, Z. W. Yin, F. Pan and L. Yang, *Angew. Chem., Int. Ed.*, 2024, **64**, e202413927.

169 X. Cui, S. Ding, Y. Niu, H. Wang, Y. Lu, Y. Hu and W. Xue, *Adv. Mater.*, 2025, 2415611.

170 S. Li, M. Jin, X. Song, S. Xu, Q. Dou, J. Zhu and X. Yan, *Energy Storage Mater.*, 2024, **73**, 103815.

171 S. Li, X. Song, P. Jing, X. Xiao, Y. Chen, Q. Sun, M. Huang, Y. Zhang, G. Li, P. Liu, S. Xu, Q. Dou, J. Zhu and X. Yan, *Adv. Funct. Mater.*, 2025, 2422491.

172 Y.-Y. Zhang, C.-H. Zhang, Y.-J. Guo, M. Fan, Y. Zhao, H. Guo, W.-P. Wang, S.-J. Tan, Y.-X. Yin, F. Wang, S. Xin, Y.-G. Guo and L.-J. Wan, *J. Am. Chem. Soc.*, 2023, **145**, 25643–25652.

173 X. Hou, T. Li, Y. Qiu, M. Jiang, H. Lin, Q. Zheng and X. Li, *ACS Energy Lett.*, 2024, **9**, 461–467.

174 Y. Li, J. Wang, Y. Wang, S. Wang, L. Wu, B. Zhou, D. Yang, L. Jiang, L. Kan, Q. Zhu, M. Kurbanov and H. Wang, *Adv. Mater.*, 2025, **37**, 2419764.

175 X. Wang, Q. Fan, Z. Liu, X. Zhu, M. Yang, Z. Guo, Y. Chen, L. Wang, Y. Jing and H. Xia, *Nat. Commun.*, 2025, **16**, 2536.

176 J. Chen, Y. Peng, Y. Yin, Z. Liu, M. Liu, Z. Fang, Y. Xie, B. Chen, Y. Cao, L. Xing, J. Huang, Y. Wang, X. Dong and Y. Xia, *Energy Environ. Sci.*, 2022, **15**, 3360–3368.

177 S. Chen, J. Fan, Z. Cui, L. Tan, D. Ruan, X. Zhao, J. Jiang, S. Jiao and X. Ren, *Angew. Chem., Int. Ed.*, 2023, **62**, e202219310.

178 Y. Yang, X. Wang, J. Zhu, L. Tan, N. Li, Y. Chen, L. Wang, Z. Liu, X. Yao, X. Wang, X. Ji and Y. Zhu, *Angew. Chem., Int. Ed.*, 2024, **136**, e202409193.

179 Y. Chen, Z. Ma, Y. Wang, P. Kumar, F. Zhao, T. Cai, Z. Cao, L. Cavallo, H. Cheng, Q. Li and J. Ming, *Energy Environ. Sci.*, 2024, **17**, 5613–5626.

180 Y. F. Tian, S. J. Tan, Z. Y. Lu, D. X. Xu, H. X. Chen, C. H. Zhang, X. S. Zhang, G. Li, Y. M. Zhao, W. P. Chen,

This journal is © The Royal Society of Chemistry 2025

Energy Environ. Sci., 2025, **18**, 6874–6898 | **6897**

Q. Xu, R. Wen, J. Zhang and Y. G. Guo, *Angew. Chem., Int. Ed.*, 2023, **135**, e202305988.

181 Y. Yue, Z. Jia, Y. Li, Y. Wen, Q. Lei, Q. Duan, J. Sun and Q. Wang, *Process Saf. Environ. Prot.*, 2024, **189**, 61–70.

182 J. Yang, M. Wang, J. Ruan, Q. Li, J. Ding, F. Fang and F. Wang, *Sci. China: Chem.*, 2024, **67**, 4063–4084.

183 J. Zhang, D. W. Wang, W. Lv, L. Qin, S. Niu, S. Zhang, T. Cao, F. Kang and Q. H. Yang, *Adv. Energy Mater.*, 2018, **8**, 1801361.

184 X. Feng, M. Ouyang, X. Liu, L. Lu, Y. Xia and X. He, *Energy Storage Mater.*, 2018, **10**, 246–267.

185 X.-B. Cheng, R. Zhang, C.-Z. Zhao and Q. Zhang, *Chem. Rev.*, 2017, **117**, 10403–10473.

186 C. K. Chan, R. Ruffo, S. S. Hong and Y. Cui, *J. Power Sources*, 2009, **189**, 1132–1140.

187 I. M. Jamesh, *J. Power Sources*, 2016, **333**, 213–236.

188 L. Mauler, F. Duffner, W. G. Zeier and J. Leker, *Energy Environ. Sci.*, 2021, **14**, 4712–4739.

189 M. S. Ziegler, J. Song and J. E. Trancik, *Energy Environ. Sci.*, 2021, **14**, 6074–6098.

190 Y. Gao, Z. Pan, J. Sun, Z. Liu and J. Wang, *Nano-Micro Lett.*, 2022, **14**, 94.

191 P. Ma, P. Mirmira, P. J. Eng, S.-B. Son, I. D. Bloom, A. S. Filatov and C. V. Amanchukwu, *Energy Environ. Sci.*, 2022, **15**, 4823–4835.

192 Y. Xue, Y. Wang, H. Zhang, W. Kong, Y. Zhou, B. Kang, Z. Huang and H. Xiang, *Angew. Chem., Int. Ed.*, 2024, **64**, e202414201.

193 D. Xia, L. Tao, D. Hou, A. Hu, S. Sainio, D. Nordlund, C. Sun, X. Xiao, L. Li, H. Huang and F. Lin, *Adv. Energy Mater.*, 2024, **14**, 2400773.

6898 | *Energy Environ. Sci.*, 2025, **18**, 6874–6898

This journal is © The Royal Society of Chemistry 2025